



RESEARCH ARTICLE

10.1029/2018JD028874

Deepti Singh and Sonali P. McDermid contributed equally to this work.

Key Points:

- Climate impacts of irrigation and land cover change are comparable in magnitude but opposite in sign over some regions, especially Asia
- Contrasting or amplifying effects of irrigation relative to land cover change extend beyond the growing season and can vary by season
- Local and remote impacts are linked to changes in moisture flux, surface and upper-level temperature gradients, and regional circulations

Supporting Information:

- Supporting Information S1

Correspondence to:

D. Singh,
deepti.singh@wsu.edu

Citation:

Singh, D., McDermid, S. P., Cook, B. I., Puma, M. J., Nazarenko, L., & Kelley, M. (2018). Distinct influences of land cover and land management on seasonal climate. *Journal of Geophysical Research: Atmospheres*, 123, 12,017–12,039.
<https://doi.org/10.1029/2018JD028874>

Received 22 APR 2018

Accepted 17 OCT 2018

Accepted article online 23 OCT 2018

Published online 10 NOV 2018

Author Contributions:

Conceptualization: Deepti Singh, Sonali P. McDermid, Benjamin I. Cook, Michael J. Puma

Investigation: Deepti Singh, Sonali P. McDermid, Benjamin I. Cook, Michael J. Puma

Methodology: Deepti Singh, Sonali P. McDermid

Resources: Sonali P. McDermid, Larissa Nazarenko, Maxwell Kelley

Writing - original draft: Deepti Singh, Sonali P. McDermid

Writing - review & editing: Deepti Singh, Sonali P. McDermid, Benjamin I. Cook, Michael J. Puma

©2018. The Authors.

This is an open access article under the terms of the Creative Commons Attribution-NonCommercial-NoDerivs License, which permits use and distribution in any medium, provided the original work is properly cited, the use is non-commercial and no modifications or adaptations are made.

Distinct Influences of Land Cover and Land Management on Seasonal Climate

Deepti Singh^{1,2} , Sonali P. McDermid^{3,4} , Benjamin I. Cook^{1,4}, Michael J. Puma^{4,5}, Larissa Nazarenko^{4,5} , and Maxwell Kelley⁴

¹Lamont-Doherty Earth Observatory, Columbia University, Palisades, NY, USA, ²School of the Environment, Washington State University, Vancouver, WA, USA, ³Environmental Studies Department, New York University, New York, NY, USA, ⁴NASA Goddard Institute for Space Studies, New York, NY, USA, ⁵Center for Climate Systems Research, Earth Institute, Columbia University, New York, NY, USA

Abstract Anthropogenic land use and land cover change is primarily represented in climate model simulations through prescribed transitions from natural vegetation to cropland or pasture. However, recent studies have demonstrated that land management practices, especially irrigation, have distinct climate impacts. Here we disentangle the seasonal climate impacts of land cover change and irrigation across areas of high agricultural intensity using climate simulations with three different land surface scenarios: (1) natural vegetation cover/no irrigation, (2) year 2000 crop cover/no irrigation, and (3) year 2000 crop cover and irrigation rates. We find that irrigation substantially amplifies land cover-induced climate impacts but has opposing effects across certain regions. Irrigation mostly causes surface cooling, which substantially amplifies land cover change-induced cooling in most regions except over Central, West, and South Asia, where it reverses land cover change-induced warming. Despite increases in net surface radiation in some regions, this cooling is associated with enhancement of latent relative to sensible heat fluxes by irrigation. Similarly, irrigation substantially enhances the wetting influence of land cover change over several regions including West Asia and the Mediterranean. The most notable contrasting impacts of these forcings on precipitation occur over South Asia, where irrigation offsets the wetting influence of land cover during the monsoon season. Differential changes in regional circulations and moist static energy induced by these forcings contribute to their precipitation impacts and are associated with differential changes in surface and tropospheric temperature gradients and moisture availability. These results emphasize the importance of including irrigation forcing to evaluate the combined impacts of land surface changes for attributing historical climatic changes and managing future impacts.

Plain Language Summary Several regions have experienced substantial agricultural expansion and intensification to meet the needs of our growing population. While the effects of land cover change associated with agriculture have been extensively studied and included as a standard forcing in simulations of historical and future climate, the influence of a common form of agricultural intensification—irrigation—is not fully understood. Despite mounting evidence of its importance on regional climate, irrigation is still not considered a standard climate forcing. To isolate the influence of irrigation from land cover changes, we conduct a suite of simulations with a state-of-the-art global climate model. Our analysis of nine regions with extensive agriculture and heavy irrigation demonstrates that irrigation has comparable climatic impacts to land cover changes. Across most regions, irrigation amplifies land cover forced changes. However, over parts of Asia, where irrigation rates are highest, irrigation contrasts land cover forced changes and the combined climate response to land cover and irrigation are opposite to what would be expected with land cover changes alone. Our results highlight the importance of including land management decisions in climate simulations for a more accurate understanding of how human activities shape climate, particularly over these regions, and have implications for management of the effects of future climate change.

1. Introduction

Agricultural activities including cropland expansion and intensification have considerably altered over 40% of the Earth's ice-free surface and have been a major source of global environmental change in the twentieth century (Defries et al., 2004; Green et al., 2005; Matson et al., 1997; Ramankutty et al., 2008; Sacks et al., 2009). While such activities have helped increase food supply globally, they have also adversely affected ecosystems and altered the regional environment (e.g., Defries et al., 2002; Mahmood et al., 2014; Matson

et al., 1997; Pielke et al., 2011). This intensification of agriculture is expected to continue in order to meet the increasing demand from a rapidly growing population (Defries et al., 2002; Tilman et al., 2001), motivating the need to better understand the environmental impacts of such activities.

A growing body of literature has focused on understanding the impacts of such activities on regional climate processes. The climatic influences of land cover changes due to cropland conversion and expansion have been extensively studied (e.g., Douglas et al., 2006; Findell et al., 2017; Mahmood et al., 2014; Pielke et al., 2011). Several studies have demonstrated the mechanisms by which land cover changes influence regional climate by altering the Earth's radiation budget and by influencing both the partitioning of surface energy fluxes and the exchange of heat and moisture between the land surface and the atmosphere (e.g., Diffenbaugh, 2009; Douglas et al., 2006; Halder et al., 2016; Hirsch et al., 2015; Lee et al., 2009; McDermid et al., 2017; Pielke et al., 2011; Quesada et al., 2017; Yamashima et al., 2015). These effects are particularly strong in regions of moderate to strong land-atmosphere coupling including South Asia, the Great Plains of North America, the Sahel, and Central and East Asia (Koster, 2004). Further, the impact of land cover changes depends on the *a priori* vegetation types (i.e., forests, shrublands, and deserts) and the local evapotranspiration regime (i.e., moisture or energy limited) and, therefore, can vary substantially across regions (Hirschi et al., 2011; Myhre et al., 2013). Despite the extensive research in this field, the timing and magnitude of the regional climate impacts of land cover changes are still uncertain (McDermid et al., 2017).

In addition to land cover impacts, land management (especially irrigation) is increasingly being recognized as a significant regional and global climate forcing in the 20th and early 21st centuries (Cook et al., 2011, 2015; Lobell et al., 2008; Lobell & Bonfils, 2008; Luyssaert et al., 2014; McDermid et al., 2017; Puma & Cook, 2010; Sacks et al., 2009; Shukla et al., 2014; Yang et al., 2016). During the twentieth century, irrigation rates have increased across many regions associated with agricultural intensification. This increase has been particularly rapid since the 1950s with the extraction of groundwater resources (Freydank & Siebert, 2008; Wada et al., 2010). Along with India, Pakistan, China, and North America, which account for over 55% of the global area equipped for irrigation, several Middle Eastern countries also had reportedly high fractions of their croplands with irrigation capabilities, based on a 2003 assessment (Freydank & Siebert, 2008). The surface temperature impacts of irrigated areas have been examined in observations and models, and the magnitude of the impacts is found to be comparable to the impacts of land cover changes alone in some regions (e.g., Luyssaert et al., 2014; Sacks et al., 2009). Despite the significance of both land cover change and irrigation as distinct external climate forcings, only a few studies have attempted to disentangle the individual effects of these external climate forcings over the historical period and existing studies are largely limited to South Asia (Douglas et al., 2006, 2009).

Several key uncertainties and limitations remain in our understanding of the climatic impacts of irrigation as a form of land management. First, it has been well documented, based on empirical and modeling evidence, that irrigation typically has a surface cooling effect across most of the tropical and midlatitude regions due to an increase in latent heat fluxes relative to sensible heating (e.g., Cook et al., 2015; Lobell et al., 2008; Lobell & Bonfils, 2008; Mueller et al., 2015, 2017; Puma & Cook, 2010; Sacks et al., 2009; Thiery et al., 2017). In contrast, however, irrigation impacts on precipitation varies widely across regions and seasons, and current understanding of these impacts is largely based on models due to limited observational studies (e.g., Cook et al., 2015; Guimbretieau et al., 2012; Im et al., 2013; Qian et al., 2013; Yang et al., 2016). For instance, irrigation enhances growing season precipitation across western North America, China, Central Asia, and the Middle East but suppresses precipitation over parts of central North America, West Africa, and South Asia (Cook et al., 2015; Douglas et al., 2009; Guimbretieau et al., 2012; Im et al., 2013; Puma & Cook, 2010; Qian et al., 2013; Saeed et al., 2009; Shukla et al., 2014; Yang et al., 2016). These studies highlight the potential for irrigation to modulate the spatial distribution of rainfall through modulating surface-atmosphere energy and moisture exchanges. While these direct effects have been examined more detailed investigations of irrigation interactions with larger-scale atmospheric circulation are still few and limited (e.g., Douglas et al., 2009; Lee et al., 2011; Shukla et al., 2014; Tuinenburg et al., 2011; Wey et al., 2015; Yang et al., 2016). Further understanding the circulation impacts will highlight ways in which land surface changes can impact climate in remote regions (de Vrese et al., 2016; Qian et al., 2013; Quesada et al., 2017).

Second, several studies have used regional climate models to investigate the effects of irrigation (e.g., Diffenbaugh, 2009; Douglas et al., 2006, 2009; Im et al., 2013; Paul et al., 2016; Saeed et al., 2009; Yang

et al., 2016). While regional models have the advantage of better simulating fine-scale processes, they do not permit a physically consistent comparison across regions. Further, typical one-way nested regional climate modeling efforts do not simulate the potential remote effects of regional land surface changes outside the simulation domain and two-way coupling is relatively rare due to its technical challenges and heavy computational requirements (Giorgi & Gutowski, 2015). Compounding this limitation, irrigation as a historical forcing is not included in the most recent archive of the Coupled Model Intercomparison Project (CMIP5; Taylor et al., 2011) despite its substantial and varying regional climatic effects (Cook et al., 2015; Pielke et al., 2011) and is still not included in many global Earth system models (Cook et al., 2015; McDermid et al., 2017). Global climate model ensembles such as the Land-Use and Climate, Identification of Robust Impacts (LUCID) project (Pitman et al., 2009) and LUCID-CMIP5 are mainly targeted at understanding the effects of land cover changes. Despite trade-offs in terms of spatial resolution, global climate simulations facilitate a comparison of the effects of forcings across regions in a physically consistent framework.

Last, only a few studies have examined how these impacts vary by season (Cook et al., 2015; Guimbertea et al., 2012; Yang et al., 2016). Changes in the timing of temperature and precipitation have implications for water availability and management, agricultural activities, biogeochemical cycles, and ecosystems (Cleland et al., 2007; IPCC, 2014; Melillo et al., 2014; Walther et al., 2002). Therefore, there is a need to better understand the underlying mechanisms by which irrigation influences regional climate, differentiate its impacts from those of land cover changes alone, and examine how these impacts vary across seasons.

With the goal of examining the independent and compound influence of these land surface forcings, we perform novel experiments with the NASA Goddard Institute for Space Studies (GISS) atmosphere-only global climate model (GCM) Model E2 (Schmidt et al., 2014) to study their effects on climate processes across regions with high agricultural intensity. Our study aims to (1) disentangle the climatic influences of land management in the form of irrigation from land cover changes, (2) identify which seasons have the strongest similarities and contrasts in climate response to these forcings, and (3) investigate the physical mechanisms associated with their differential impacts. By demonstrating the impacts of irrigation as comparable to those of land cover-induced changes, our study highlights the importance of considering irrigation forcing in addition to land cover change to capture the complete influence of land surface changes on historical climate. Although land use and land cover change is a standard historical forcing in the CMIP5 (Taylor et al., 2011) and CMIP6 (Eyring et al., 2016), irrigation is still not included despite its increasing recognition as a global climate forcing. However, its inclusion in the Land Use Model Intercomparison Project-CMIP6 will facilitate a comparison and a mechanistic understanding of the relative effects of land cover and irrigation on regional climate and inform more meaningful comparisons of their effects across models. With the continued intensification of agriculture (Foley et al., 2011), insights from this study will also facilitate better land management and inform climate mitigation efforts in the coming decades (Hirsch et al., 2017; Seneviratne et al., 2018).

2. Data and Methods

2.1. GISS ModelE2 and Irrigation Implementation

We use an updated and intermediate version of the NASA GISS ModelE2 GCM (hereafter ModelE2), which utilizes vegetation characteristics from the Ent Terrestrial Biosphere Model (Ent TBM). ModelE2 is a major Earth system model that contributes to the CMIP5 (Eyring et al., 2015) as an ongoing development effort, with the most recently documented version, ModelE2 R/H (where R and H refer to different ocean models), described in Miller et al. (2014), Nazarenko et al. (2015), and Schmidt et al. (2014). ModelE2 runs at $2^\circ \times 2.5^\circ$ spatial resolution with 40 vertical layers in the atmosphere (model top at 0.1 hPa), where resolution is enhanced between 825 hPa and the tropopause. We note that ModelE2 produces slightly warmer temperatures over South Asia, slightly cooler temperatures over the midlatitudes, higher precipitation over parts of the midlatitudes, and lower precipitation over South Asia (Schmidt et al., 2014; Shukla et al., 2014). Despite these biases, ModelE2 simulated climatologies of temperature, precipitation, and circulation, and their responses to historical anthropogenic forcings are in general agreement with observations and observed trends (Miller et al., 2014; Schmidt et al., 2014; Shukla et al., 2014). Further, because we are comparing simulated responses within a physically consistent model framework, these biases will be

Table 1

Summary of Land Surface Properties of the Nine SREX regions—Average Crop Fraction (Values Range From 0 to 1), Area Average Height of the Dominant Vegetation Type and Maximum LAI in NatVeg and Crops scenarios, Maximum Irrigation Rate, and Albedo Change in the Crops Scenario Relative to NatVeg

| SREX regions | Average crop fraction | Avg height of dominant veg type in NatVeg (m) | Avg height of dominant veg type in Crops (m) | Maximum LAI NatVeg (m^2/m^2) | Maximum LAI Crops (m^2/m^2) | Maximum irrigation ($\times 10^9 m^3/m^2$) | Albedo change |
|--------------|-----------------------|-----------------------------------------------|----------------------------------------------|----------------------------------|---------------------------------|----------------------------------------------|---------------|
| CAM | 0.50 | 10.30 | 6.50 | 1.70 | 2.60 | 1.80 | 0.01 |
| CAS | 0.67 | 1.40 | 0.80 | 0.30 | 0.50 | 6.80 | -0.01 |
| CEU | 0.53 | 15.60 | 7.90 | 2.50 | 3.10 | 0.40 | 0.06 |
| CNA | 0.72 | 9.50 | 4.90 | 1.80 | 3.60 | 1.30 | 0.02 |
| EAS | 0.54 | 12.60 | 8.10 | 1.70 | 2.60 | 2.50 | 0.01 |
| MED | 0.53 | 8.80 | 4.70 | 1.30 | 2.10 | 3.00 | 0.00 |
| SAS | 0.50 | 8.60 | 5.10 | 1.10 | 2.00 | 11.40 | 0.01 |
| TIB | 0.57 | 1.30 | 0.70 | 0.30 | 0.30 | 1.00 | 0.00 |
| WAS | 0.46 | 1.40 | 0.90 | 0.20 | 0.70 | 1.90 | -0.03 |

Note. SREX = Special report on Managing the Risks of Extreme Events and Disasters to Advance Climate Change Adaptation; LAI = leaf area index; CAM = Central America/Mexico; CAS = Central Asia; CEU = Central Europe; CNA = Central North America; EAS = East Asia; MED = South Europe/Mediterranean; SAS = South Asia; TIB = Tibetan Plateau; WAS = West Asia.

generally consistent across simulations. We utilize the noninteractive atmospheric compositions, prescribed ocean version of the model to evaluate equilibrated, climatological surface-atmosphere dynamics.

The Ent TBM is used in the *biophysics-only* mode, in which water vapor fluxes are prognostically simulated for each grid box by a prescribed canopy structure and maximum and minimum leaf area index (LAI), which are given for 17 possible Plant Functional Types (PFTs; Kim et al., 2015). Further details about the natural vegetation phenology and about canopy radiative transfer can be found in Kim et al. (2015) and Friend and Kiang (2005), respectively. The Ent TBM is forced by atmospheric and land surface variables obtained from ModelE2 and the embedded land surface model (Aleynov & Schmidt, 2006; Puma et al., 2013; Rosenzweig & Abramopoulos, 1997). Vegetation albedo is prescribed per extrapolations from (Matthews, 1983) land cover classifications and mapped to Ent PFTs (Friend & Kiang, 2005).

To represent the LAIs for natural vegetation cover only, ModelE2 utilizes a monthly prescribed value and annual maximum taken from the Moderate Resolution Imaging Spectroradiometer (MODIS; MCD12Q1 V005 L3) International Geosphere-Biosphere Program land cover types for the year 2004 (Friedl et al., 2010). All crop cover classes, defined as a managed C3 grasses PFT, were set to 0 fractional coverage such that the regionally prevailing land cover classes occupied the entirety of the grid box. The MODIS LAI is assigned by the land cover fraction of the grid box, taking the LAI value assigned to particular PFT and multiplying that by the fractional coverage for the same PFT. The sum of the fractional land cover per grid box is always 1, while the sum across the PFTs' LAIs is equal to the maximum LAI. Within the model simulations, the 2004 MODIS monthly prescribed LAI are linearly interpolated to create a daily time series.

2.2. Land Cover and Irrigation Data

Land cover change-only experiments leverage the global distribution of general crop and pasture coverage developed by Pongratz et al. (2008) and Hurt et al. (2011). These data sets contain crop and pasture cover for every 50 years from 800 to 1850, for each decade between 1850 and 1985, and then annually for 1986 to present. We run our experiments using the crop coverage for the year 2000 only (i.e., not time varying). To accommodate crop cover, natural vegetation and bare soil cover are rescaled proportionally with the crop PFT such that all cover fractions sum to 1 in a grid box. Modern agricultural LAIs were represented by merging a global map of maize, rice, wheat, and soy distributions (Monfreda et al., 2008) with crop-specific maximum LAI from the MODIS-derived LAI3g product (Zhu et al., 2013). This approach quantifies these crops' maximum LAI at a fine spatial resolution, accounting for areas where multiple crops may be grown within a single grid box, and then scales up their merged behavior into one crop cover type at the ModelE grid box scale. Only grid cells that were mostly cropped (>80%) were included. In many regions, crop cover replaces a large proportion of the natural vegetation. For example, across western and southern Asia (which comprise one of our focus domains described below), approximately 50% of total land was converted to cropland, constituting a substantial regional forcing (supporting information Figure S1 and Table 1).

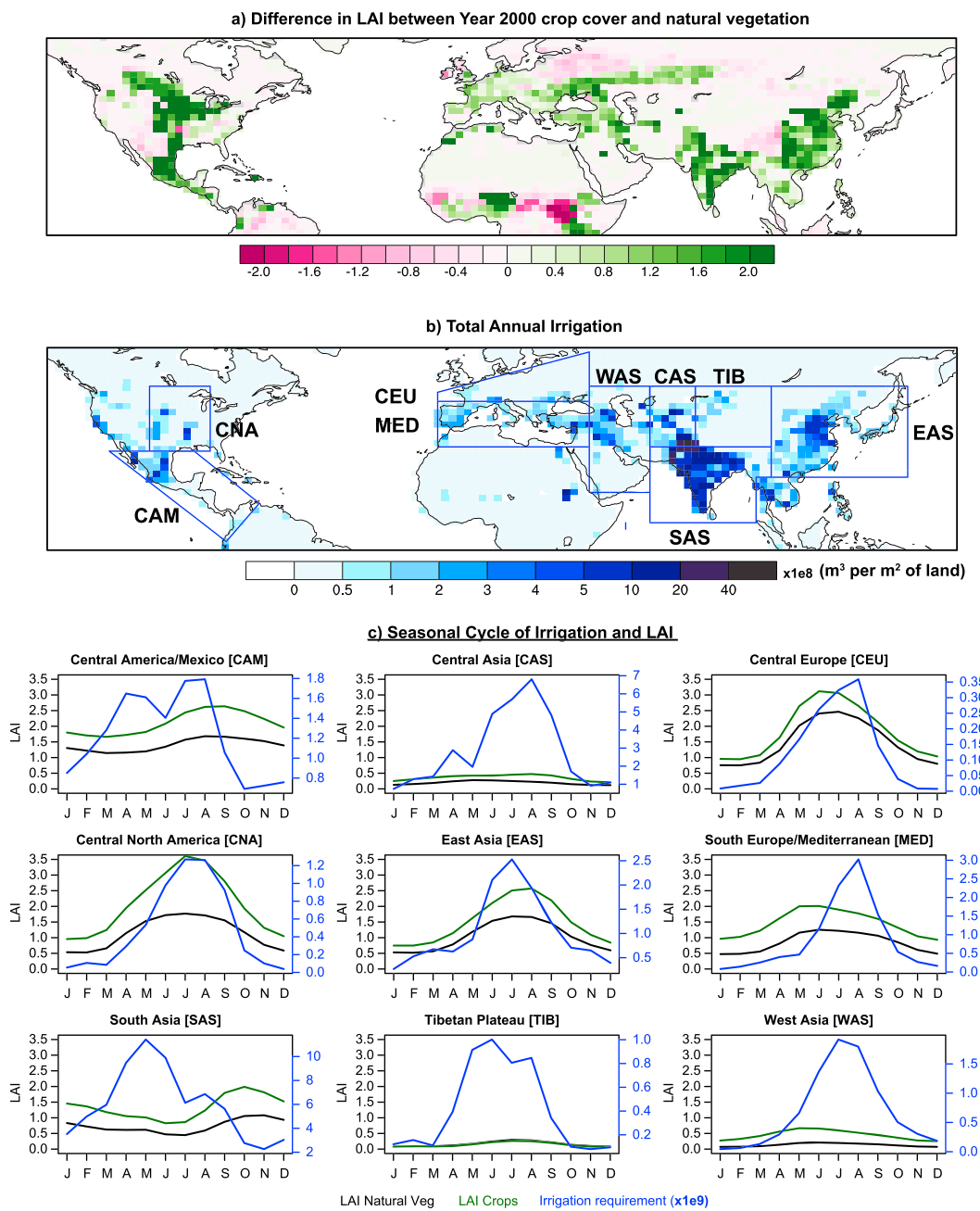


Figure 1. (a) Difference in leaf area index (LAI) of crops and natural vegetation in the simulations for September as a representative example, (b) total annual irrigation requirements, and (c) seasonal cycle of irrigation and LAI in the nine SREX regions. Note: The scales of irrigation requirements in panel (c) vary by region to account for the substantial regional differences in magnitude. Further, the regional average LAI in West Asia, Central Asia, and Tibet are small due to the relatively large fraction of bare soil in these regions. LAI = leaf area index; SREX = Special report on Managing the Risks of Extreme Events and Disasters to Advance Climate Change Adaptation.

For simulations also evaluating the impact of agricultural land management, we focus specifically on modern irrigation and both its extent and intensity (Figure 1b). We use prescribed global irrigation rates in ModelE2, which is implemented as detailed in Puma and Cook (2010). In summary, these rates were calculated offline using a water balance model approach that considers interactions between human water use (e.g., agriculture, industry, and households) and terrestrial water fluxes and, in particular, is responsive to crop and agricultural water demands (Wada et al., 2014). This dynamic modeling approach is combined with empirical data sets of irrigation-equipped areas and provides estimates of historical irrigation amounts. Calculations

of irrigation rates from the offline model avoids unrealistic amounts that might otherwise arise from calculations within the GCM due to ModelE2 biases in simulating climate variables, particularly precipitation. Further, its finer resolution enables a more accurate representation of crops and, therefore, their water requirements. To be consistent with the above described crop coverage, we use irrigation amounts prescribed for the year 2000, assigning monthly values from Wada et al. (2014) to the middle of each month and linearly interpolating to the daily level. Irrigation amounts are applied to the entire vegetated portion of the grid cell, as the model does not have distinct soil columns for natural vegetation and crops, which may lead to overestimates in the spatial extent of applied irrigation water within some grid cells (although the total volume of applied irrigation is consistent with Wada et al., 2014). We also note that the gross irrigation estimates are used rather than the estimates of the irrigation water used by the crops (i.e., net irrigation), so that the runoff, infiltration, and water uptake physics of ModelE2 can determine how much irrigation water is transpired by vegetation.

2.3. Experiment Design

To compare the effects of agricultural land cover and land management, we conduct three 70-year, constant-forcing simulations with the GISS ModelE2, using preindustrial radiative forcings and prescribed climatological (1876–1885) sea surface temperatures from the Hadley Centre Global Sea Ice and Sea Surface Temperature dataset (Rayner et al., 2003). These simulations, differing only in their surface cover and excluding any other external climate forcings, are designed to isolate the seasonal climate responses to different land surface scenarios while accounting for natural atmospheric variability rather than to explain historical changes. The first simulation includes only natural vegetation cover, which we use as the baseline for comparison of land surface changes (referred to as NatVeg). The second simulation, representing agricultural expansion, is run with static modern-day crop cover (Figure S1) based on year 2000 estimates in order to evaluate the impacts of land cover change alone (referred to as Crops). In the third simulation, representing one form of agricultural intensification, we include static, year 2000 irrigation rates in addition to year 2000 crop cover to evaluate the combined impacts of applying irrigation to agricultural areas (referred to as IrrigatedCrops). While these simulations are aimed at isolating the response of agriculture-driven land cover change and irrigation, irrigation only occurs over cropped areas and therefore is not an orthogonal climate forcing to land cover change. The seasonal cycle of natural vegetation, crop cover, and irrigation is included in these simulations. To account for model spin-up time, we only use the last 50 years of the simulations for the analysis.

For analyzing the change in seasonality of climate variables in response to different surface conditions, we focus on 9 of the 26 subcontinental regions defined in the Intergovernmental Panel on Climate Change Special report on Managing the Risks of Extreme Events and Disasters to Advance Climate Change Adaptation (SREX; Seneviratne et al., 2012). While there is substantial spatial variability in climate variables within these large domains, these regions are widely used for comparing the response of climatic variables to various external forcings (e.g., Greve et al., 2018; Hirsch et al., 2017; Kharin et al., 2018; Seneviratne et al., 2012; Thiery et al., 2017), providing a standard set of domains for future comparisons across models. The boundaries of these nine regions—Central America/Mexico (CAM), Central Asia (CAS), Central Europe (CEU), Central North America (CNA), East Asia (EAS), South Europe/Mediterranean (MED), South Asia (SAS), Tibetan Plateau (TIB), and West Asia (WAS)—are shown in Figure 1. These are the subset of regions that have relatively high modern-day irrigation rates and are characterized by intensive agricultural production (Figures 1a and 1b). The exception is TIB, which is included due to its proximity to the heavily irrigated regions in Asia. The seasonal cycle of irrigation requirements in the IrrigatedCrops scenario along with the LAI in the NatVeg and Crops scenarios in each region is shown in Figure 1c. We calculate area-weighted averages of surface temperature and precipitation over land within these regions.

The land surface properties and irrigation rates of these regions are summarized in Table 1. The average cropped fraction across the nine SREX regions varies from 0.45 over WAS to 0.72 over CNA (Figure S1 and Table 1). Although crops replace a variety of vegetation types, crops lower the average vegetation heights over all the study regions (Table 1), with implications for reduced roughness lengths. Across the nine SREX regions, the model LAI—an indicator of plant growth—is higher for crops relative to natural vegetation (Figure 1a and Table 1). The LAI typically peaks during the boreal summer season, except in SAS and CAM, where the peak LAI occurs in the fall season (Figure 1c). Irrigation rates vary substantially between these regions, with the heaviest rates over SAS (Figure 1b and Table 1). Within these regions, there is

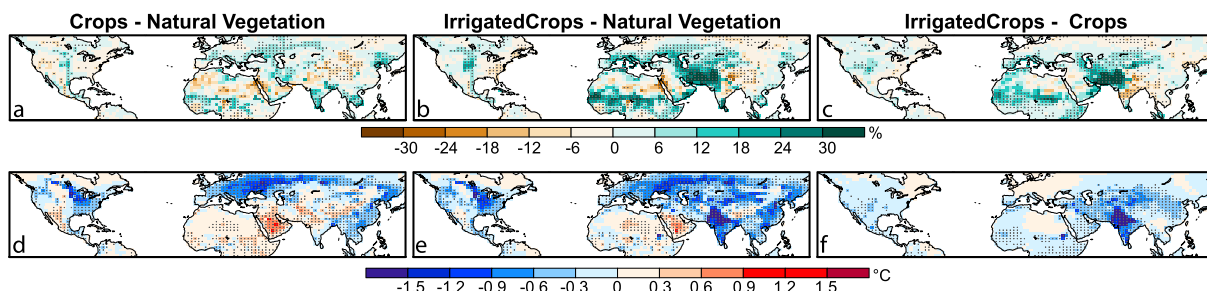


Figure 2. Simulated changes in (a–c) total annual precipitation and (d–f) annual mean surface temperature in the agricultural land cover change experiment relative to the natural vegetation experiment (Crops – Natural Vegetation), in agricultural land cover change with added irrigation experiment relative to the natural vegetation experiment (IrrigatedCrops – Natural Vegetation), and in the agricultural land cover change with added irrigation relative to the land cover change only experiment (IrrigatedCrops – Crops). Stippling indicates that changes are significant at the 5% level.

considerable variation in the seasonal cycle of irrigation requirements (Figure 1c). For instance, the peak irrigation in SAS occurs during the premonsoon and early-monsoon season, whereas the peak in other regions occurs during the primary growing season of June–September. Because irrigation is applied in most months of the year and crop growth in some regions peaks following the boreal summer season, the climatic responses to these forcings (i.e., land cover change and applied irrigation) could extend to multiple seasons beyond the primary growing season.

3. Results

Here we contrast the climate responses across the nine SREX regions to these forcings, which are representative of the effects of agricultural land conversion and agricultural intensification, relative to a climate with natural vegetation. Since external forcings are identical for the length of the simulation, the year-to-year differences only represent the internal atmospheric variability in the *forced* response to different surface conditions. For the forced climate response to land cover change or irrigation, we calculate the difference in the mean climate across 50 years of the Crops and IrrigatedCrops scenarios relative to the NatVeg scenario. To estimate the statistical significance of the distribution of differences between each set of scenarios, we apply the two-sided Student's *t* test.

3.1. Annual and Seasonal Temperature and Precipitation Impacts

On an annual scale, agriculture-driven land cover change (Crops-NatVeg) significantly enhances precipitation in many agricultural areas with the exception of TIB and northern SAS (Figure 2a). Over the regions that experience precipitation increases associated with agriculture, addition of irrigation enhances this amplification of precipitation with the largest effects—increases of 18–24% relative to land cover forced changes—over WAS (Figures 2b and 2c). However, over other regions that experience precipitation declines associated with agriculture, addition of irrigation to croplands leads to competing changes in precipitation relative to those induced by agricultural land cover change alone, either dampening the land cover-induced changes or causing changes of the opposite sign (Figures 2a and 2c). Over much of CAS, TIB, and northern SAS where crop cover-induced changes were negative or insignificant, addition of irrigation causes relative increases in precipitation of >30% (Figures 2b and 2c). In contrast, over peninsular India, irrigation causes a relative reduction in annual precipitation of 12–18% where land cover changes alone increase precipitation (Figures 2a and 2c).

Similarly, these land surface forcings also have opposite influences on annual mean surface temperatures over some regions, including parts of CAM, WAS, CAS, and northern SAS (Figures 2d–2f). While land cover change alone leads to warming of between 0.3 and 0.9 °C in these regions, the addition of irrigation largely masks this warming and instead has a uniform cooling effect (Figures 2d and 2e). The relative cooling effect exceeds -1.5°C over the heavily irrigated parts of northern SAS and CAS (Figure 2f). In contrast, the impacts of these forcings are similar in sign over much of TIB and EAS, where irrigation amplifies the cooling effect of crops by 0.3–0.6 °C.

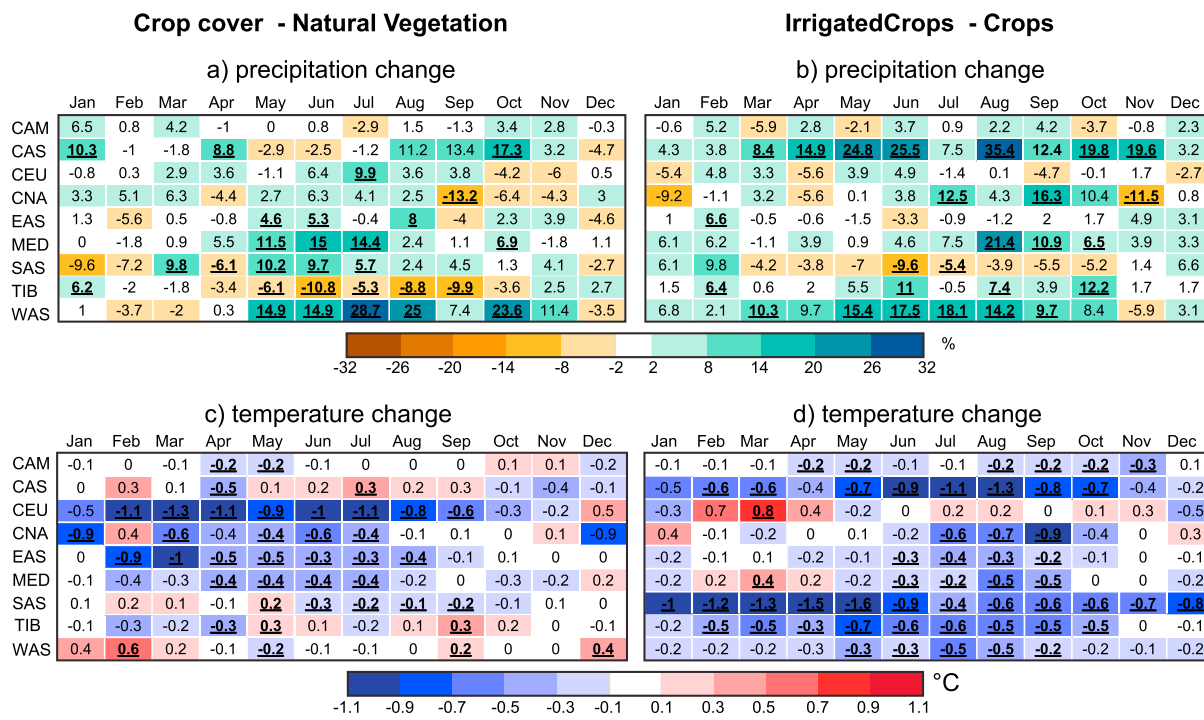


Figure 3. Simulated changes in monthly, area-average (a, b) precipitation and (c, d) surface temperature in the agricultural land cover change experiment (Crops) relative to the natural vegetation experiment (NatVeg) and the agricultural land cover change with added irrigation experiment (Irrigated Crops) relative to Crops. Refer to Figure 1 for regions. Changes that are underlined and in bold are significant at the 10% level.

Although the impacts of temperature are largely similar across seasons, precipitation impacts vary considerably in magnitude and direction (Figures S2 and S3). To characterize their effects by season, we quantify the area-weighted average monthly temperature and precipitation changes in the two forcing scenarios relative to the Natural Vegetation scenario for each of the nine regions (Figure 3). The amplifying and contrasting effects of irrigation on land cover-induced changes are more prominent on the monthly time scale. Among these regions, the effects of both forcings vary by season, and significant changes also occur outside the primary growing season. The most significant precipitation increases in response to land cover changes occurs over SAS during the premonsoon and monsoon seasons (March–July) and over MED and WAS during late spring, summer, and fall (May–October; Figure 3a). During these seasons, irrigation amplifies land cover-induced precipitation increases over WAS by ~10–18% and over the MED by ~4–20% in different months (Figures 3a and 3b). In addition, irrigation causes large and significant increases in precipitation over CAS, with the magnitudes varying between 8% and 35% in different months (Figure 3b). SAS is the most prominent example of the contrasting influence of these forcings, where the addition of irrigation opposes the land cover forced precipitation increases with relative reductions of between 5% and 10% during the premonsoon and summer monsoon months, leading to little overall change in precipitation in response to the combined forcings (Figure 3b). In addition, irrigation also weakens the land cover change induced precipitation declines during most seasons except winter over TIB and in September–October over CNA and reverses the negative precipitation response to land cover during the winter over SAS (Figures 3a and 3b). The effects of irrigation are relatively small and less consistent in other regions.

To further assess the relative importance of irrigation to the annual hydrological balance, Table 2 shows the annual precipitation (P), evapotranspiration (ET), and added irrigation water across our focus regions. Also shown are differences in these quantities (P and ET) from the NatVeg experiment. Irrigation reduces annual P – ET most substantially in SAS, CAM, and CAS. While both precipitation and ET increase over CAM and CAS, P – ET reductions result from higher ET increases relative to precipitation. In SAS, however, annual precipitation does not undergo a substantial change (and is actually slightly reduced), while ET significantly increases. Across the other regions, however, annually added irrigation water does not substantially alter P – ET (as

Table 2

Annual Precipitation (P), Evapotranspiration (ET), and Added Irrigation (All in Millimeters per Year) in the IrrigatedCrops Scenario

| SREX regions | Precipitation (P) | ΔP | Evapo-transpiration (ET) | ΔET | $P - ET$ | $\Delta P - \Delta ET$ | Added irrigation water |
|--------------|-----------------------|------------|------------------------------|-------------|----------|------------------------|------------------------|
| CAM | 1370.27 | 24.35 | 1093.07 | 69.29 | 277.2 | -44.94 | 39.42 |
| CAS | 450.94 | 55.94 | 385.03 | 95.08 | 65.92 | -39.14 | 91.43 |
| CEU | 902.3 | 12.71 | 606.27 | 4.93 | 296.03 | 7.78 | 3.79 |
| CNA | 816.82 | 19.28 | 669.82 | 41.64 | 147.01 | -22.37 | 15.67 |
| EAS | 1026.22 | 16.17 | 698.19 | 42.67 | 328.03 | -26.5 | 33.46 |
| MED | 893.7 | 72.52 | 758.23 | 65.52 | 135.47 | 6.99 | 27.54 |
| SAS | 1262.9 | -7.9 | 794.77 | 187.97 | 468.13 | -195.87 | 193.57 |
| TIB | 527.57 | 0.64 | 401.62 | -1.69 | 125.95 | 2.33 | 13.23 |
| WAS | 367.02 | 39.24 | 410.97 | 38.25 | -43.95 | 0.99 | 22.02 |

Note. Changes (Δ) in precipitation and ET in IrrigatedCrops relative to the NatVeg scenario are also provided. SREX = Special report on Managing the Risks of Extreme Events and Disasters to Advance Climate Change Adaptation; LAI = leaf area index; CAM = Central America/Mexico; CAS = Central Asia; CEU = Central Europe; CNA = Central North America; EAS = East Asia; MED = South Europe/Mediterranean; SAS = South Asia; TIB = Tibetan Plateau; WAS = West Asia.

averaged over these regions). These annual results are consistent with our above described seasonal findings across these regions, particularly where irrigation negates land cover-induced changes.

In contrast to the mixed precipitation responses, irrigation largely causes cooling relative to land cover-induced changes in most seasons (Figures 3c and 3d). The most robust changes in response to land cover occur in the spring and early part of the growing seasons. Land cover changes lead to strong and robust cooling over CEU from February to August (~0.8–1.3 °C), EAS from February to August (0.4–0.9 °C), and CNA from March to July (0.4–0.6 °C) and moderate cooling in some seasons in other regions where crops replace denser forest cover (Figure 3c). However, land cover change leads to moderate warming over CAS and TIB in May–September (0.2–0.3 °C) and WAS in December–February (0.4–0.6 °C), where cropping occurs on areas of sparse vegetation (Figure 3c). With added irrigation, there is significant cooling across most regions and seasons with a few exceptions, such as the relative warming effect over CEU during February–March (Figure 3d). Peak cooling in most regions generally tends to co-occur with the timing of the peak irrigation rates. The strongest effect of irrigation occurs over SAS, with cooling of 1–1.5 °C during January–May when the effects of land cover are insignificant and amplifies the land cover-induced cooling by 0.4–0.9 °C in the remaining months (Figure 3d). In addition, irrigation causes significant cooling over CNA, EAS, WAS, and the MED, amplifying the effects of land cover change, and reverses the warming associated with land cover change over CAS and TIB, during the height of the growing season (June–September; Figures 3c and 3d).

3.2. Influence on Surface Energy Balance and Partitioning

To understand the causes of amplifying or contrasting impacts of irrigation relative to land cover change on surface climate, we examine their influence on the net radiative fluxes at the surface and their energy partitioning into latent and sensible heat fluxes, which ultimately influence surface climate. Net surface radiative flux is defined as the sum of the net shortwave and longwave radiation at the surface. We evaluate changes in these quantities during the three seasons with the most significant changes and contrasts between the two scenarios—spring (March–April–May), summer (June–July–August), and fall (September–October–November) (Figures 4 and 5).

Land cover changes considerably alter the net surface radiation across the nine study regions and also lead to a repartitioning of surface energy between sensible and latent heat fluxes over parts of SAS and WAS (Figures 4a–4c and 5a–5c). Changes in land cover from natural vegetation to crops largely lead to decreases in net surface radiation except over WAS, CAS, and parts of the MED. The largest and most widespread decreases in surface radiation occur over CNA, CEU, and EAS in spring and summer and parts of SAS and TIB in all three seasons (Figures 4a–4c). These changes are not restricted to the main agricultural areas. These declines in net surface radiation along with small but significant decreases in the Bowen ratio, indicating an increased partitioning of fluxes into latent heat, are associated with surface cooling relative to the

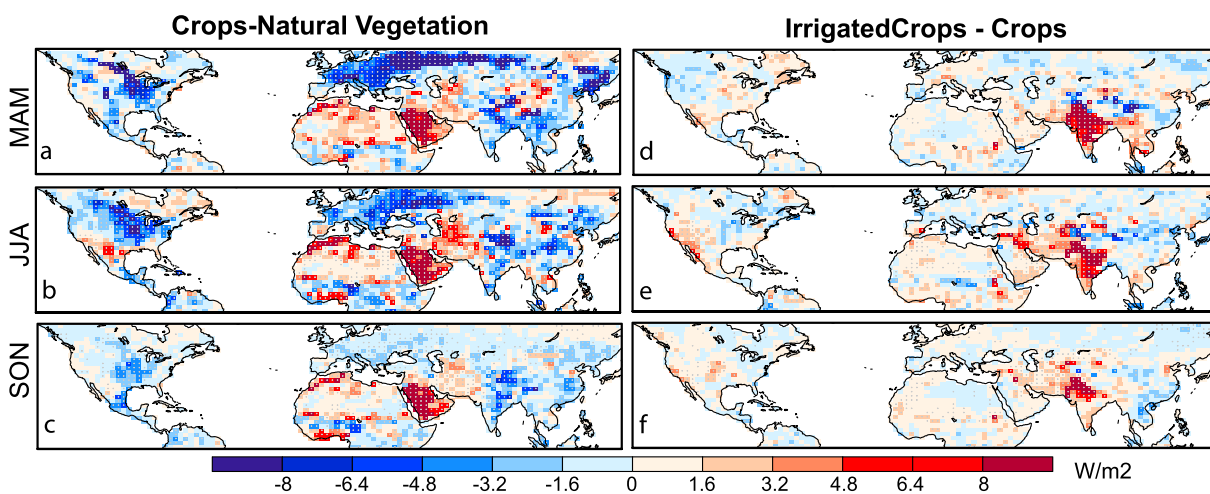


Figure 4. Simulated changes in seasonal average net radiative flux at the surface in the (a–c) agricultural land cover change experiment relative to the natural vegetation experiment (Crops – Natural Vegetation) and (d–f) the agricultural land cover change with added irrigation experiment relative to the land cover change experiment (Irrigated Crops – Crops). Stippling indicates that changes are significant at the 5% level. MAM = March–April–May; JJA = June–July–August; SON = September–October–November.

natural vegetation state in most regions (Figures 5a–5c and S2). The exception is northern SAS in spring, where despite little change in net surface radiation, increases in Bowen ratio (enhanced sensible heat fluxes relative to latent heat fluxes) are associated with surface warming (Figures 4, 5a, and S2a). In contrast, net surface radiation increases by $>8 \text{ W}/\text{m}^2$ over WAS during all three seasons and by $4.8\text{--}6.4 \text{ W}/\text{m}^2$ over CAS in summer despite varied changes in the Bowen ratio, leading to robust surface warming in these regions (Figures 4a–4c, 5a–5c, and S2).

The contrasting effects of irrigation on surface temperature can be explained by its influence on the net surface radiation and Bowen ratio. The starker contrast in net surface radiation changes between the two scenarios is over SAS. Particularly over the heavily irrigated regions of SAS, irrigation leads to large increases in net surface radiation that contrast the negative impacts of land cover changes alone (Figures 4d–4f). Across much of SAS, CAS, and WAS, enhanced soil moisture associated with irrigation increases latent heat fluxes and reduces the Bowen ratio (Figures 5d–5f). Despite the increases in net surface radiation, these significant and large decreases in Bowen ratio associated with relative increases in latent heat fluxes overwhelm the

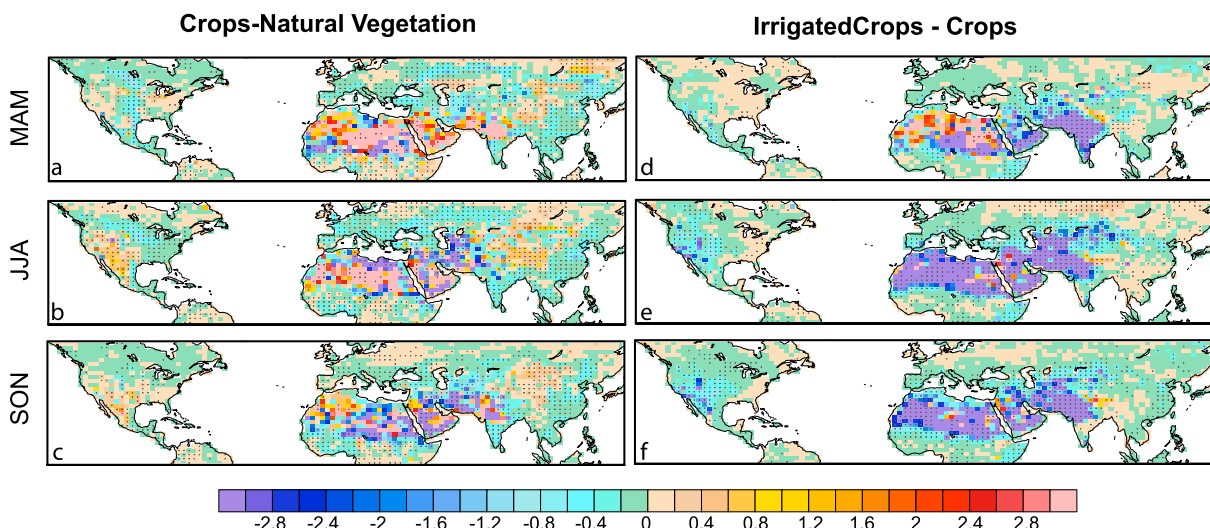


Figure 5. Same as in Figure 4 but for Bowen ratio, which is the ratio of sensible to latent heat fluxes.

contrasting effects of land cover changes to cause relative cooling over these regions (Figures 3 and S2). These effects are strongest and most widespread during the spring and summer, when the irrigation rates are highest but persist into the fall over some areas. Associated with peak irrigation rates during the main growing season, irrigation also leads to significant decreases in the Bowen ratio due to an increase in latent heat fluxes and consequential cooling over CAS, WAS, and the MED (Figures 5k and 5l). These changes occur in the two other seasons as well but are less widespread. Over other regions, irrigation effects on surface energy fluxes are relatively small.

To further understand the influence of these land surface forcings on net surface radiation in the two scenarios, we examine the changes in surface shortwave and longwave components in a subset of SREX regions that experience the largest changes or contrasting responses of land cover change and irrigation (Figure 6). Land cover changes mainly alter surface radiation through changes in shortwave fluxes, whereas irrigation, and the resulting Bowen ratio changes, mainly decreases upward longwave radiation (LWUP) due to its surface cooling effect. In CAS, WAS, and the MED, where land cover changes cause an increase in net surface radiation in most seasons, the increases are largely associated with changes in shortwave fluxes with relatively small changes in longwave fluxes in all seasons except the summer. Decrease in albedo due to crops replacing areas of sparse vegetation (Table 1) lead to decreases in outgoing shortwave radiation (OUTSW) in all three seasons in WAS, and summer and fall in CAS and the MED, with smaller decreases in incoming shortwave radiation (INSW). The addition of irrigation amplifies the net surface radiation (NET) changes in all three regions, with the largest changes during the peak growing season. Enhanced cloud cover with irrigation (Figure S4) leads to decreases in INSW and increases in downward longwave radiation over these regions. LWUP also decreases due to surface cooling. Therefore, the decreases in INSW are compensated by the resulting net increases in surface longwave radiation, contributing to enhance NET over these regions.

Changes over CNA and SAS contrast these patterns. Over CNA where crops replace denser forest vegetation (albedo increases; Table 1), crops have the opposite effect of increasing OUTSW and therefore reducing NET, but changes in other fluxes vary by season (Figures 6d–6f). INSW decreases in the summer along with decreases in LWUP, but the opposite changes occur in the fall. Irrigation amplifies the changes in shortwave and longwave radiation in the summer and reverses the land cover forced changes in fall. Over SAS, land cover forced changes are relatively small but irrigation effects are among the strongest across all five regions (Figures 6j–6l). Substantial surface cooling associated with irrigation leads to large decreases in LWUP in the region for all three seasons, increasing net radiation and overwhelming the contrasting response associated with land cover change. Coincident with the timing of peak irrigation, the largest changes are found in spring (Figure 6j). Similar to other regions, enhanced atmospheric moisture and cloud cover reduces INSW over SAS in spring (Figures 6j and S4). However, the opposite effect occurs in the summer, the only season with substantial declines in cloud cover, contributing to the overall increase in NET (Figures 6j, 6k, and S4).

3.3. Influence on Thermodynamics, Circulation, and Tropospheric Temperatures

While changes in surface energy balance and partitioning of surface fluxes are relevant for understanding the first-order effects on local climate, changes in the atmospheric dynamics and thermodynamics are also important in shaping local and remote climate impacts (Figures 7 and 8). This is evidenced from the substantial changes in tropospheric temperature and circulation in response to land cover change and irrigation. The temperature effects of both land surface forcings are not restricted to the surface. We find significant changes extending to the lower (850 hPa) and upper tropospheric (300 hPa) levels in all three seasons (Figures 7 and 8). Overall, the effects of irrigation relative to land cover changes on lower tropospheric temperatures are consistent with the surface temperature effects (Figures 7d–7f). However, the relative effects of irrigation on upper tropospheric temperatures are more variable. There is evidence of remote impacts, and in some regions, irrigation-induced upper-level atmospheric changes contrast those at the surface (Figure 8). For instance, cooling of similar magnitude to the surface occurs in the lower troposphere over the heavily irrigated parts of SAS in all three seasons. Most prominently in the summer, the effects of irrigation also extend into the upper troposphere with widespread cooling ($>1^{\circ}\text{C}$) over CAS, WAS, and parts of the MED (Figures 8c and 8d). However, these temperature effects vary by season. For instance, relative to land cover forced changes, springtime irrigation causes upper tropospheric warming over SAS of a small but significant amount (0.2–0.4 $^{\circ}\text{C}$) and cooling of a similar magnitude over much of the high latitudes. Such changes in tropospheric

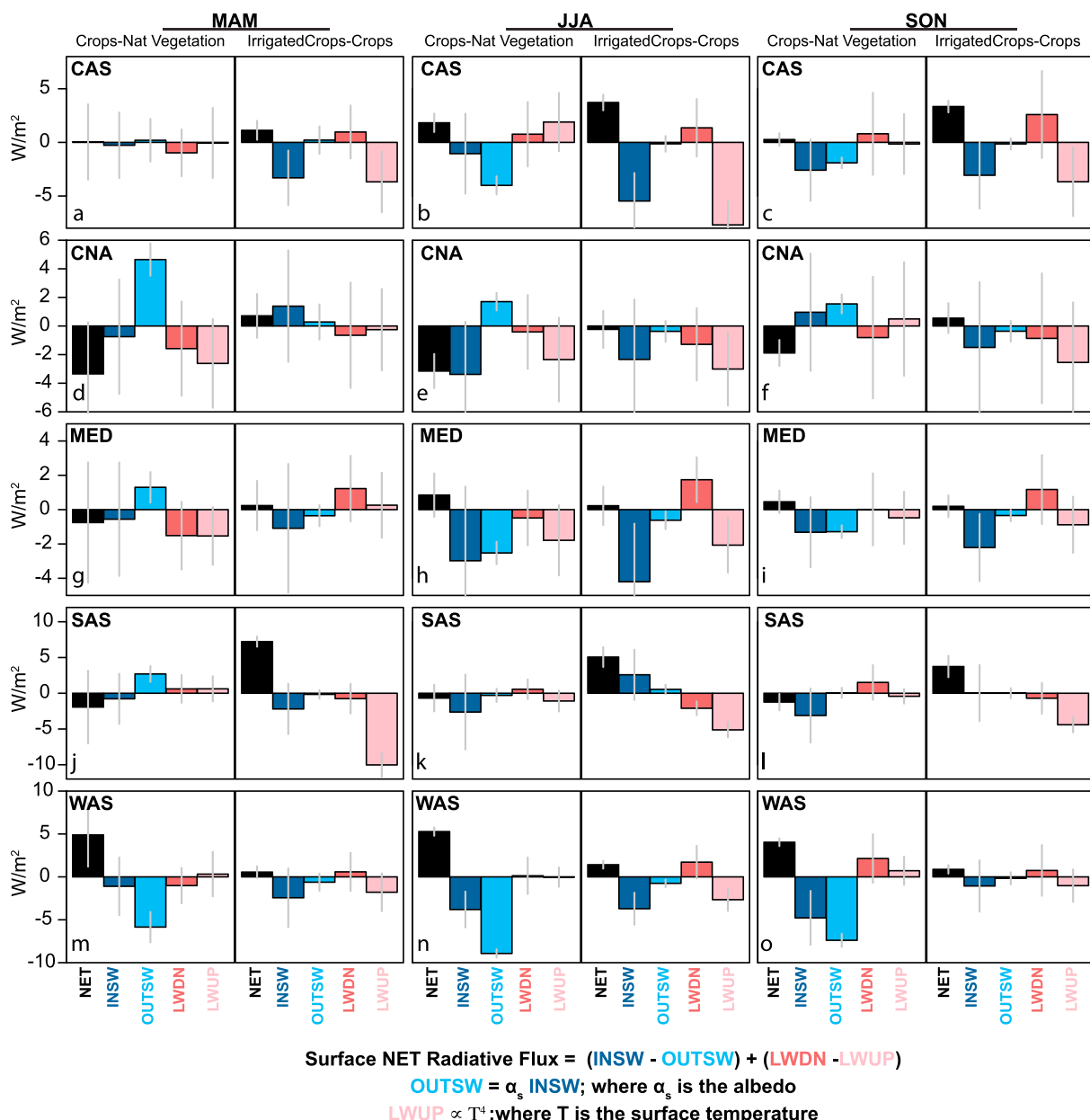


Figure 6. Seasonal decomposition of regional average changes in net radiative flux at the surface (NET) into its shortwave and longwave components at the surface—incoming shortwave (INSW), outgoing shortwave (OUTSW), downward longwave (LWDN), and upward longwave (LWUP) radiation—in the agricultural land cover change experiment relative to the natural vegetation experiment (Crops – Natural Vegetation) and the agricultural land cover change with added irrigation experiment relative to the land cover change experiment (IrrigatedCrops – Crops). OUTSW is related to the INSW by the surface albedo (α_s). LWUP is proportional to the surface temperature (T). Gray lines on the bar plots indicate the $\pm 0.5\sigma$ range around the mean changes. MAM = March-April-May; JJA = June-July-August; SON = September-October-November; CAS = Central Asia; CNA = Central North America; MED = South Europe/Mediterranean; SAS = South Asia; WAS = West Asia.

temperatures influence the horizontal and vertical temperature gradients that affect atmospheric stability and circulation patterns and in turn affect the processes that control the distribution of precipitation and other climate parameters (e.g., Adam et al., 2014; Biasutti et al., 2018; Lee et al., 2011; Yang et al., 2016; Zhang et al., 2016).

We also find notable impacts of crop cover and irrigation on the regional circulation, with the most prominent differences over Asia (Figure 9). Irrigation and land cover changes have opposing effects on the circulation and moisture convergence over SAS in all three seasons, consistent with their opposing influences on

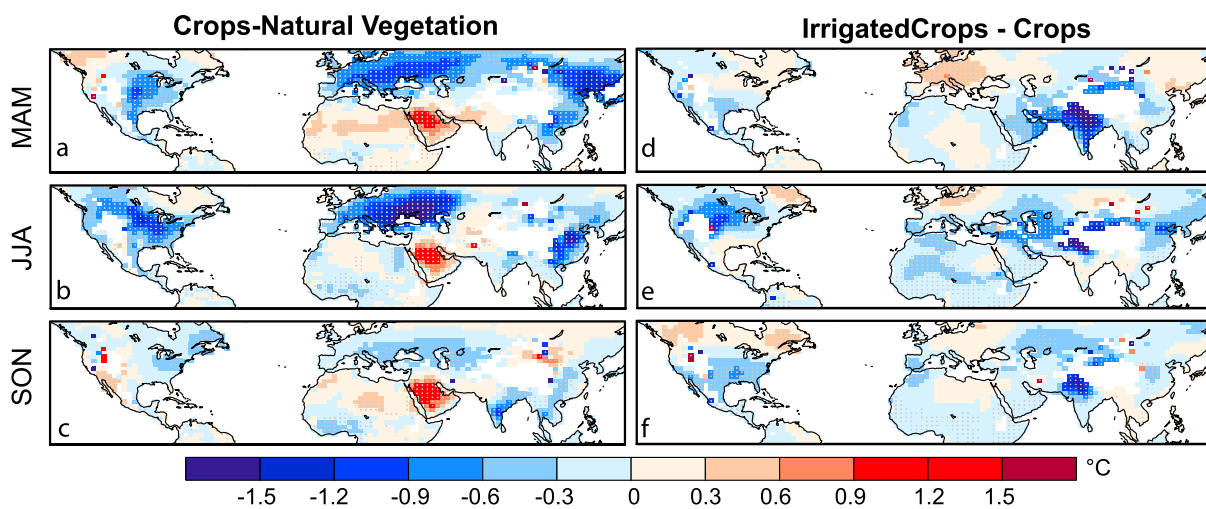


Figure 7. Same as in Figure 4 but for lower tropospheric temperature (850 hPa). Stippling indicates changes that are significant at the 5% level.

precipitation (Figures 3 and 9). Low-level (850 hPa) moisture convergence is closely associated with seasonal rainfall over these regions. Land cover changes enhance the South Asian summer monsoon circulation and cause an increase in moisture convergence during summer and fall, consistent with the increased rainfall in those seasons (Figures 9a–9c). In contrast, irrigation leads to widespread divergence and anomalous easterly flow in these seasons across most of SAS, where suppressed convergence is consistent with the drying, except over the northwestern parts (Figures 2a–2c and 9d–9f). Although the changes are smaller in comparison, there are similarly competing changes from land cover and irrigation on the summer monsoon circulation and moisture convergence over EAS.

Amplifying effects of irrigation relative to land cover changes on the circulation and moisture convergence are observed over WAS, CNA, and the MED, consistent with their precipitation responses (Figure 9). Over WAS, irrigation amplifies the land cover-induced low-level (850 hPa) convergence over the Arabian Peninsula mainly in the summer season. While there is relatively little irrigation over the Arabian Peninsula, these large circulation changes are indicative of the remote effects of irrigation, potentially a response to the larger-scale modulation of temperature gradients by heavier irrigation in the northern part of WAS or a response to the substantial circulation anomalies associated with irrigation over SAS. Similar enhancing effects of irrigation are seen on moisture convergence over the MED mainly in the fall, when the strongest

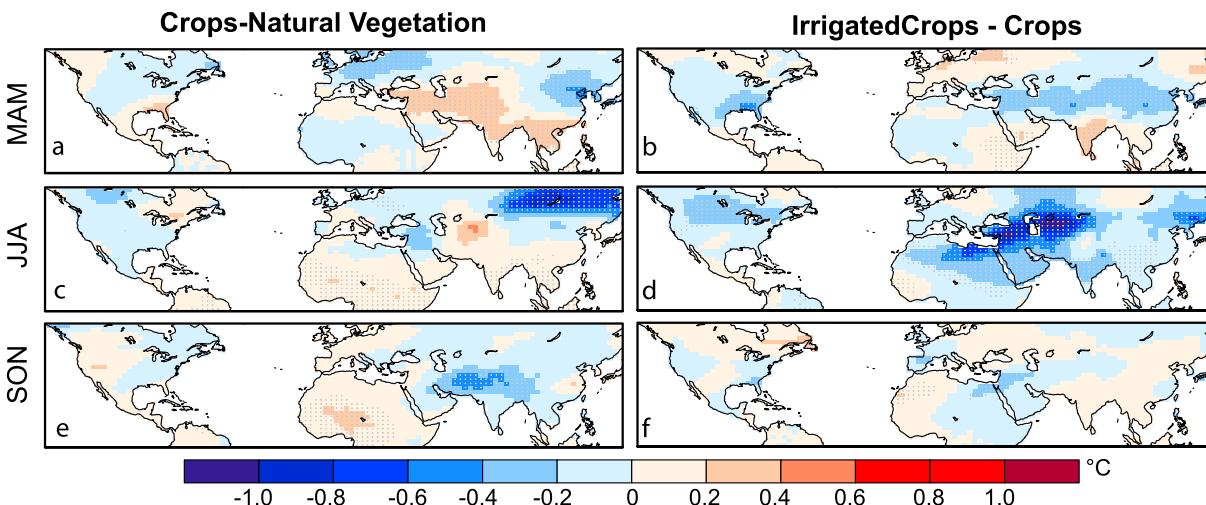


Figure 8. Same as in Figure 4 but for upper tropospheric temperature (300 hPa).

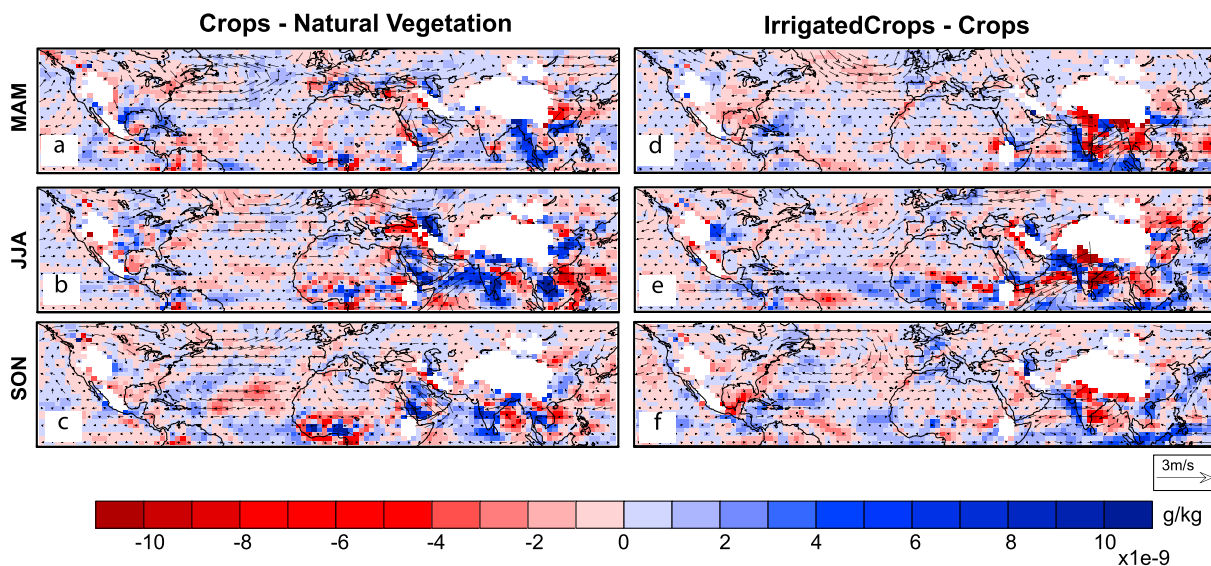


Figure 9. Same as in Figure 4 but for low-level (850 hPa) moisture convergence. Arrows represent the 850-hPa wind anomalies.

precipitation increases occur in response to irrigation. This occurs through anomalous westerly flow over much of the region. Such similarities and differences in the circulation changes provide a mechanism to explain the amplifying and contrasting precipitation responses over these regions.

Further, while the large-scale circulation changes influence regional moisture convergence, other factors can influence convective activity and, therefore, precipitation responses to forcings (Figure 10; Banacos & Schultz, 2005). We examine changes in moist static energy (MSE), a quantity closely associated with precipitation, particularly in the tropics and over monsoon regions. Associated with surface warming and enhanced moisture

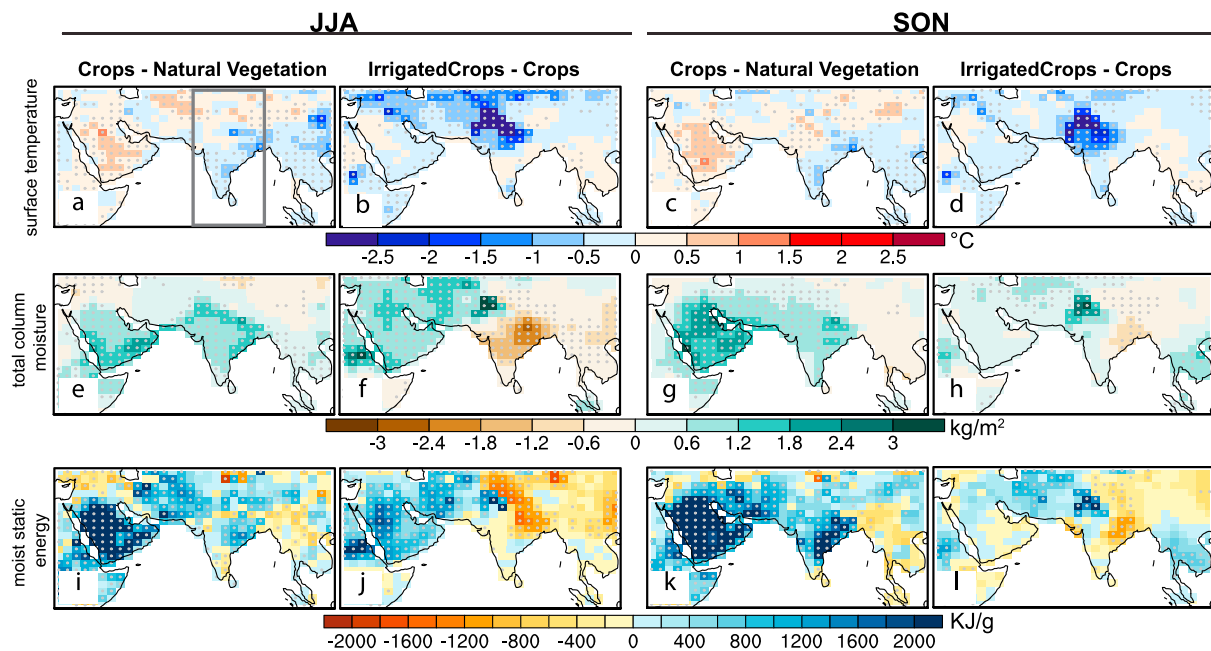


Figure 10. Simulated changes in seasonal (a–d) surface temperature, (e–h) total column moisture, and (i–l) moist static energy in the agricultural land cover change experiment relative to the natural vegetation experiment (Crops – Natural Vegetation) and the agricultural land cover change with added irrigation experiment relative to the land cover change experiment (Irrigated Crops – Crops). Stippling indicates that changes are significant at the 5% level. JJA = June–July–August; SON = September–October–November. Gray box in panel (a) encloses the region within 70–90°E used for calculating the longitudinal averaged winds and humidity across South Asia in Figures 11 and 12.

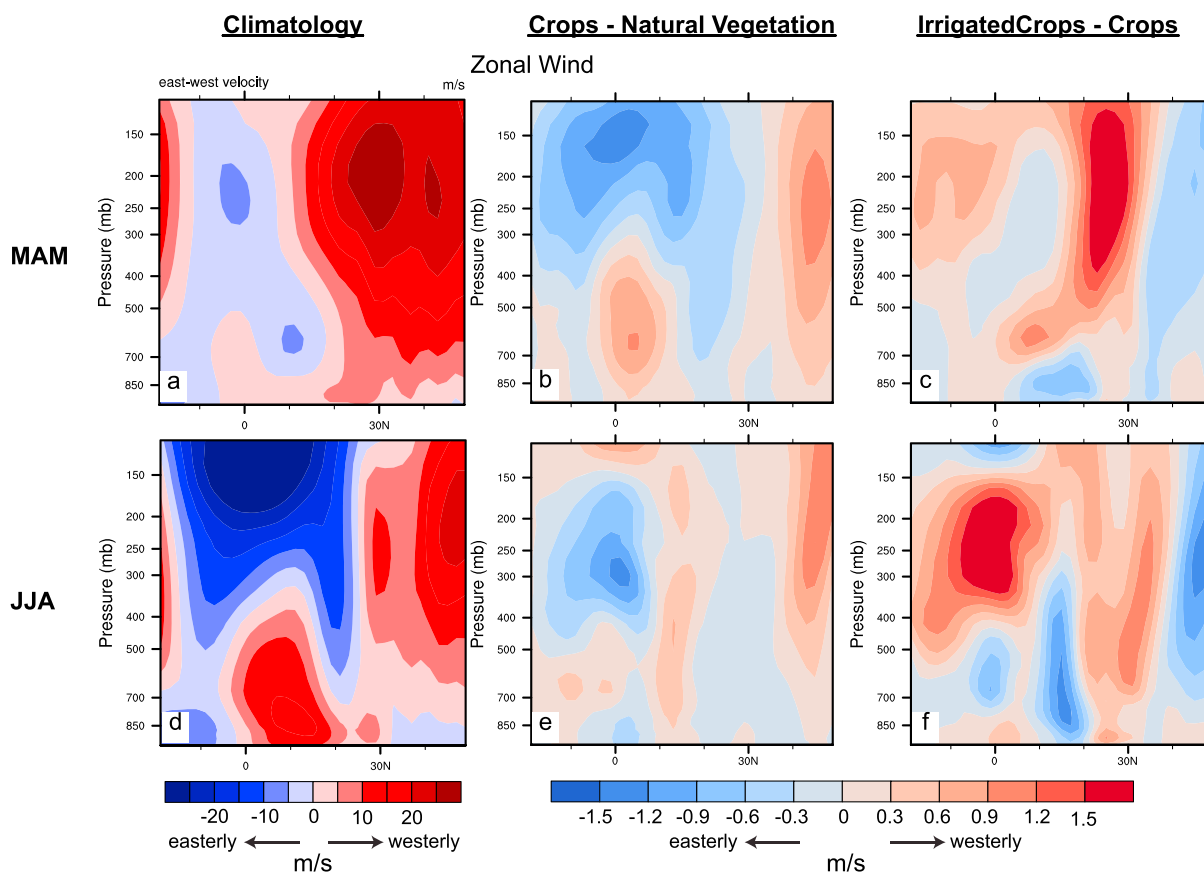


Figure 11. Seasonal (a,d) climatology and (b–c, e–f) changes in zonally averaged winds across South Asia ($70\text{--}90^{\circ}\text{E}$; see gray box in Figure 10a) in the agricultural land cover change experiment relative to the natural vegetation experiment (Crops – Natural Vegetation) and the agricultural land cover change with added irrigation experiment relative to the land cover change experiment (Irrigated Crops – Crops). MAM = March-April-May; JJA = June-July-August.

availability, land cover changes enhance MSE across much of SAS and WAS, particularly in the summer and fall. Irrigation amplifies MSE over WAS with the most widespread changes in the summer, which contribute to the enhancement of rainfall during the primary growing season (Figure 10j). However, irrigation causes strong relative declines in MSE over parts of SAS due to the opposite temperature and moisture effects during all three seasons that are sufficiently strong to reverse the land-induced MSE changes, except over the northwestern parts where it acts in concert with land cover-induced changes. These regions are coincident with the regions of contrasting and amplifying precipitation responses to these forcings over SAS (Figures 2 and 10).

3.4. Impacts on the Spring and Summer Circulation Over SAS

Given the strongest influence on the low-level circulation over SAS relative to the rest of the domain (Figure 11), we delve deeper into understanding the contrasting responses of land cover and irrigation on the circulation over SAS (Figure 11). During spring, strong upper-level westerly flow persists over northern SAS, which has an influence on precipitation over northern and northeastern SAS (Tyagi et al., 2012). Land cover changes lead to a northward shift in the climatological westerlies over the region, which is linked to declines in precipitation over these regions (Figure S2). Irrigation causes a contrasting southward shift and a strengthened circulation, which enhances precipitation over these South Asian subregions (Figure S2). In addition, irrigation contributes to increases in low-level (up to 700 hPa) moisture availability, which do not occur with land surface changes alone (Figures 12a–12c), further supporting the relative enhancement of rainfall over northern SAS in contrast to the decline in response to land cover alone during spring. Winter season circulation and precipitation responses to these forcings are similar to the spring season changes (Figures S3 and S5).

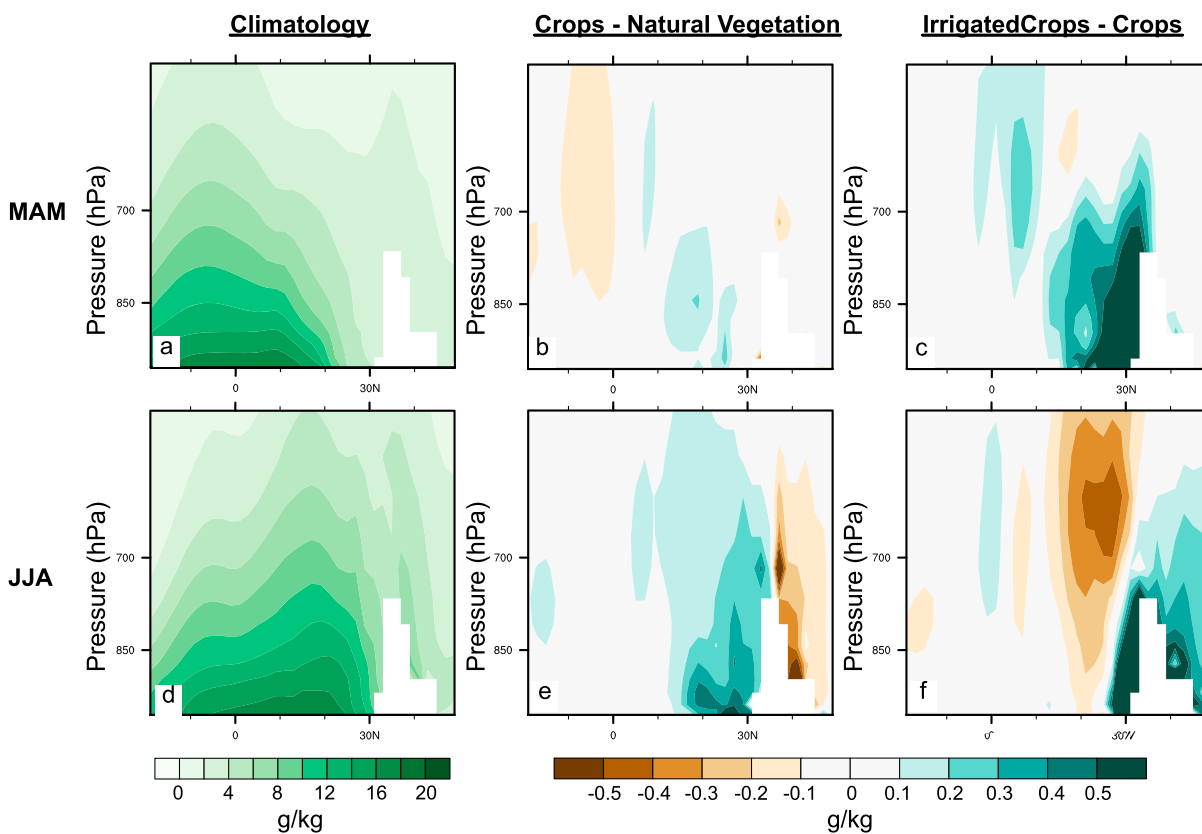


Figure 12. Same as in Figure 11 but for moisture availability (specific humidity).

During the summer season, the circulation reverses and is associated with westerly flow in the lower troposphere and easterly flow in the upper troposphere (Figure 11d). Both agricultural land cover change and irrigation are associated with enhanced moisture availability along northern SAS, with much greater enhancement at the surface and lower troposphere with the latter (Figures 12d–12f). This enhancement is mainly concentrated in the northern regions associated with widespread agricultural land cover change and intensification along the Indo-Gangetic Plain. While the circulation response to land cover change is largely restricted to a slight strengthening of the upper-level easterly jet over the ocean, the response to irrigation is a weakening at the upper and lower levels, indicative of a weakened monsoonal circulation over SAS (Figures 11d–11f). The weakened circulation but enhanced moisture availability in response to irrigation has competing effects on the monsoon, with the weakened circulation slightly outweighing the latter, leading to weaker summer monsoon rainfall across most of SAS except the northwest. Over the northwestern part, the increased lower level moisture availability has a downstream wetting influence where it is in concert with the land cover forced changes (Figures 2a–2c and 9e).

Annual $P - ET$ is reduced over SAS (Table 2), owing to substantial ET increases and relatively little changes in annual precipitation. However, our current circulation analysis indicates enhanced moisture divergence (Figure 9) and reduced circulation strength (Figure 11) during the monsoon season, when the region typically receives the majority of its annual precipitation. When combined, these results suggest that while irrigation reduces the monsoonal moisture transport over SAS, enhanced ET resulting from the substantial added irrigation water may recycle moisture to maintain much of the annual precipitation amount. However, we further note that despite little overall change in SAS-averaged precipitation, its spatial distribution is substantially changed (Figure 2). Precipitation is locally enhanced over the most heavily irrigated regions, while precipitation deficits manifest over much of peninsular India (Figures 2 and S2).

In addition to local changes, such changes in moisture availability and circulation also have impacts in remote regions that need to be considered. Enhanced moisture fluxes from the surface could also lead to increased upper tropospheric temperatures through diabatic heating such as over SAS in spring (Figures 8a and 8b). In

addition, in both spring and summer seasons, irrigation influences the zonal wind strength by up to 7% in the midlatitudes (north of 25°N). Such changes can have downstream effects, such as over EAS. In addition, enhanced low-level moisture availability over northern SAS can be linked to the enhancement of moisture transport over the WAS and CAS (Figure 9). While the current suite of simulations does not tease apart the local versus remote effects, the strong precipitation enhancement over these regions despite comparably low irrigation rates suggests the potential for substantial remote effects.

4. Discussion

The impacts of irrigation and land cover change on climate have been widely studied in regional (e.g., Diffenbaugh, 2009; Douglas et al., 2009; Im et al., 2013; Kueppers et al., 2007; Lobell et al., 2008; Niyogi et al., 2010; Paul et al., 2016; Shukla et al., 2014; Yang et al., 2017) and global contexts (e.g., Cook et al., 2011; Cook et al., 2015; Feddema et al., 2005; Guimbarteau et al., 2012; Puma & Cook, 2010; Sacks et al., 2009). While studies have examined the overall climatic effects of irrigated croplands, to the best of our knowledge, their effects have not been contrasted against each other on a global scale. Given the recent studies that have identified irrigation as a strong forcing on regional climate (e.g., Cook et al., 2011, 2015; Im et al., 2013; Puma & Cook, 2010; Sacks et al., 2009; Thiery et al., 2017), its importance relative to, and its interaction with, land cover changes is still uncertain. While both crop cover and irrigation have increased over recent decades, their trajectories may diverge in the future with a likely intensification of agriculture and a slowdown of agricultural expansion (Matson et al., 1997). In some regions, declining freshwater and groundwater resources might limit irrigation water availability and necessitate reversion to rain-fed agriculture (Elliott et al., 2014). These implications are particularly interesting where irrigation-induced climate responses oppose those of land cover change alone. In intensively cultivated SAS, for example, large amounts of added irrigation water may offset winter and spring precipitation declines resulting from land cover changes alone (Figure S3). This suggests that, notwithstanding trends in other anthropogenic forcings, land cover change-induced precipitation declines may accompany reduction irrigation intensity. Therefore, understanding their individual influences is important not only in the context of attributing historical climate change but also for projecting and managing future impacts (Hirsch et al., 2017; McDermid et al., 2017).

We compare and contrast the climatic effects of agricultural land conversion and intensification across nine heavily irrigated regions of the world. Coincident with the highest irrigation rates and most extensive agricultural expansion, the strongest surface and atmospheric changes in response to these forcings occur over Asia during multiple seasons. Land cover change alone can cause regional warming despite being an overall negative global forcing (Myhre et al., 2013). Irrigation combined with land cover change has a strong cooling effect in most regions, consistent with previous findings (e.g., Cook et al., 2015; McDermid et al., 2017; Sacks et al., 2009; Thiery et al., 2017), that is sufficiently strong to reverse these positive temperature changes. For instance, irrigation causes 2–3 times as much cooling over much of Asia as the simulated land cover forced warming (0.3–0.6 °C; Figure 2). This implies that neglecting the effect of irrigation would lead to underestimating the effect of land surface changes on historical climate. In the future, the lack of irrigation due to water shortage in vulnerable parts of Asia, which are already experiencing rapid depletion of groundwater and freshwater resources (Elliott et al., 2014; Rodell et al., 2009), could result in amplified warming in currently irrigated croplands.

In contrast to the largely consistent cooling effect on temperature, irrigation has varied effects on precipitation across different regions (Figures 2 and 3). Though the largest impacts of irrigation occur during the main growing season across the regions considered here, there are also considerable effects on precipitation in the spring and fall season across parts of Asia. Over most regions, irrigated croplands tend to enhance primary growing season precipitation in addition to the effect of land cover changes alone. However, over SAS and CAS, the influence of irrigation opposes the wetting influence of land cover change only during the summer monsoon season and is sufficiently strong to reverse the direction of changes. The relative weakening effect of irrigation on the Indian summer monsoon rainfall is consistent with previous studies (Cook et al., 2015; Douglas et al., 2009; Guimbarteau et al., 2012; Shukla et al., 2014). However, the magnitude of this effect found in our study is smaller than that found in Douglas et al. (2009) and Guimbarteau et al. (2012), potentially due to differences in climate models, spatial resolutions, physical representation of irrigation in the studies, and experimental designs. Consistent with Guimbarteau et al. (2012) and Shukla et al. (2014),

precipitation declines occur primarily due to decreases in total column moisture over most of India and weakening of the circulation with irrigation, which are in contrast to the land cover forced changes. This circulation weakening leads to reduced low-level convergence, which along with reduced MSE have a drying effect on precipitation despite an increase in moisture availability. This is in contrast to the moderate surface warming and enhanced convergence over the region induced by land cover changes alone.

The differences in surface temperature response are largely due to the different impacts of land cover change and irrigation on the partitioning of surface fluxes into latent and sensible fluxes (Figure 5). The contrasting, but comparable, impacts of irrigation and land cover change on surface energy partitioning at a global scale are similar to the findings over India in Douglas et al. (2009). In addition to substantial changes in energy partitioning, irrigation also considerably increases NET, which enhances surface energy availability over the heavily irrigated parts of Asia, reversing the effect of land cover changes (Figures 4 and 5). The contrasting responses of NET in these experiments arise from land cover changes modulating shortwave fluxes through albedo changes and irrigation modulating shortwave and longwave fluxes through enhanced near-surface moisture and surface cooling (Figures 6, 12, and S4). Our results indicate that irrigation-induced cooling reduces LWUP over most regions, and the associated enhancement of near-surface atmospheric moisture and cloud cover increases downward longwave radiation and decreases incoming shortwave radiation over some regions, consistent with the findings of Cook et al. (2015).

Several other factors can affect regional precipitation, and these can vary by season. Beyond Lee et al. (2011) and Zhang et al.'s (2016) demonstration of the impacts of land cover changes on tropospheric temperatures, our study shows that the impacts of irrigation also extend into the upper atmospheric levels and can be different from near-surface changes (Figures 7 and 8). The differing temperature responses at the upper levels and the surface such as over SAS in spring are likely linked to diabatic heating associated with enhanced moisture fluxes that extend into the lower to mid troposphere (Figures 9 and 12). Large-scale changes in the horizontal and vertical temperature gradients in the atmosphere can influence regional precipitation patterns by altering circulation patterns and atmospheric stability to a greater extent than changes in moisture availability. We demonstrate such substantial effects of irrigation relative to land cover on low-level circulation, moisture convergence, and MSE (Figures 9–12). For instance, over SAS, despite increases in moisture availability due to irrigation, the weakening of the circulation, associated with changes in the meridional thermal gradient and reduction in MSE, leads to negative impacts on summer monsoon rainfall in contrast to land cover changes. In other regions, irrigation substantially amplifies land surface influences on the larger-scale circulation and, thus, its subsequent precipitation. Such impacts of irrigation are also seasonally dependent. For example, while our results show that irrigation leads to a weakening of the summer monsoon circulation over SAS, Wey et al. (2015) show that irrigation-induced near-surface cooling leads to a strengthening of the winter monsoon circulation (also see Figure S5).

Such changes to the circulation can affect climate in remote regions in addition to local impacts through temperature and moisture advection. Some examples of such potential remote or downstream effects in other regions are also noted in several studies (Mahmood et al., 2014; Perugini et al., 2017; Pielke et al., 2011; Yang et al., 2016), including by Zhang et al. (2016) for tropospheric temperature impacts in response to land cover changes and by Lo and Famiglietti (2013) for precipitation in response to irrigation addition. In our study, the strong enhancement of rainfall over parts of WAS and CAS that are not colocated with the heaviest irrigation rates are likely the remote effects of the enhancement of moisture convergence from the irrigated areas of SAS. In addition, the relatively large changes in surface temperatures over CAS and TIB, and in upper tropospheric temperatures over the MED, CAS, and WAS, also highlight such remote effects. While changes in the primary growing season are associated with widespread irrigation across multiple regions, winter season changes are largely a response to irrigation over SAS. Wey et al. (2015) show that the remote impacts of this wintertime irrigation over SAS can extend into the midlatitudes as far as North America, where it affects surface climate through a deepening of the Aleutian Low. (Though not shown, our simulations show a similar response of irrigation relative to land cover changes alone). Together, these results indicate the importance of considering land cover change and land management as distinct forcings over irrigated and nonirrigated areas.

Our analysis also demonstrates that the individual and relative regional effects of crop cover and irrigation can vary considerably by season. For instance, changes from natural vegetation to croplands cause

significant surface warming over WAS in the winter months but have a negligible effect in the summer season when vegetation growth typically peaks. However, the strongest cooling effect of irrigation over this region occurs during the spring and summer months. In addition, irrigation has a relative warming effect during February–April over the MED but a relative cooling effect during most other months. Similarly, over SAS, irrigation has a drying effect relative to land cover change on rainfall during May–September but has a small wetting in winter months. Given these varying effects, our results underscore the importance of considering the impacts of land cover change and irrigation across multiple seasons and not just the primary growing season (Ge, 2010; Raddatz, 2007).

Our findings are based on simulations with a single GCM and with realistic but time-invariant forcings. While this allows us to clearly identify the climatic responses to these forcings, this design poses some important limitations to the conclusions of this study. First, there are limitations in the model representation of irrigation and crops. Irrigation is potentially overestimated in the current model since the irrigation module applies irrigation to an entire vegetated fraction of the grid cell even if it is only partially cropped (Cook et al., 2015; Puma & Cook, 2010; Shukla et al., 2014). Model development efforts targeted at improving the representation of these processes are required for a better understanding of the impact of these forcings. Second, different models have different land surface representations, parameterizations, irrigation schemes, and biases, which could result in differing simulated responses to these surface changes (e.g., Boisier et al., 2012; de Noblet-Ducoudré et al., 2012; Lawrence et al., 2016; Pitman et al., 2009; Quesada et al., 2017). Although LUCID allowed for such comparisons of the land cover change effects, this ensemble is still limited compared to the suite of CMIP5 models. The new set of simulations that will be part of the Land Use Model Intercomparison Project contribution to CMIP6 (Lawrence et al., 2016) could help address this limitation. Third, the coarse model resolution likely does not capture the spatial heterogeneity in the surface forcings considered here and important fine-scale interactions and feedbacks and potentially overestimates irrigation at the grid scale. Although some studies have employed regional climate models for such assessments, higher-resolution GCMs are needed for comparing these effects across regions and capturing the potential remote effects highlighted in this study and previous studies. Fourth, the isolated transient climate response could likely be different than the equilibrium climate response that is examined here. In the real world, these forcings occur along with other external forcings such as greenhouse gases and aerosols that could modulate the response to these surface forcings. Therefore, the interactions of these land surface forcings with other anthropogenic climate forcings need to be further disentangled and investigated.

5. Conclusions and Implications

We highlight four main conclusions from our study of nine regions with heavy irrigation and extensive agricultural land conversion. First, the effects of irrigation on surface temperature and precipitation are comparable to or larger in magnitude than the effects of land cover changes. Second, over some regions, irrigation amplifies the effects of land cover changes (such as for precipitation over parts of the MED and WAS) but in other regions it either dampens or reverses them (e.g., temperature and precipitation changes over parts of SAS). Third, irrigation impacts are not restricted to the primary growing season or peak irrigation season and can vary by season. Fourth, the impact of these forcings and their amplifying and contrasting effects extends into the troposphere and to remote regions. Changes in the vertical distribution of moisture and in-cloud cover in response to these forcings influence temperatures at the lower atmospheric levels and throughout the troposphere in some regions. These changes in the tropospheric temperatures and low-level moisture availability influence atmospheric circulation patterns. Consequently, through changing atmospheric circulations, irrigation and land cover change can affect climate in remote regions.

Our study highlights the importance of land management decisions on regional climate relative to land cover change alone and has implications for better planning and management. Furthermore, it is becoming increasingly clear that such human activities have played a role in shaping historical climate changes. Most detection and attribution studies—including the new Detection and Attribution Model Intercomparison Project-CMIP6 (Gillett et al., 2016)—and historical simulations do not consider the role of land management when simulating historical anthropogenic forcings. The substantial magnitude of climatic impacts in heavily irrigated areas suggests that these experiments are potentially missing a substantial historical climate forcing in certain regions that could lead to biases in simulating historical climate change and incomplete attribution

of historical changes to anthropogenic activities. We argue that the individual effects of irrigation forcing should be considered in addition to land use forcing, as they have distinct controls. Especially when land cover and land management decisions are being considered based on their potential for climate change mitigation (Hirsch et al., 2017; Seneviratne et al., 2018; Wilhelm et al., 2015), there is an urgent need to better understand their individual influences on regional climate processes in the past and future, which also requires a better understanding of their interaction with other anthropogenic forcings.

Data Availability

Results here are based on ModelE tag modelE_AR5_v2_branch, which is an intermediate version of the GISS ModelE2 and is available in the development repository (https://simplex.giss.nasa.gov/cgi-bin/gitweb.cgi?p=modelE.git;a=tag;h=refs/tags/modelE_AR5_v2_branch). All the input files and simulation output are available at 10.5281/zenodo.1402171.

Acknowledgments

D. Singh was supported by the Lamont-Doherty Earth Observatory Fellowship. B. I. Cook and M. J. Puma (for development of irrigation in ModelE) were supported by the NASA Modeling, Analysis, and Prediction program. Resources supporting this work were provided by the NASA High-End Computing (HEC) Program through the NASA Center for Climate Simulation (NCCS) at Goddard Space Flight Center. All authors declare no conflicts of interests.

References

- Adam, O., Schneider, T., & Harnik, N. (2014). Role of changes in mean temperatures versus temperature gradients in the recent widening of the Hadley circulation. *Journal of Climate*, 27(19), 7450–7461. <https://doi.org/10.1175/JCLI-D-14-00140.1>
- Alleinov, I., & Schmidt, G. A. (2006). Water isotopes in the GISS ModelE land surface scheme. *Global and Planetary Change*, 51(1-2), 108–120. Available at: <http://www.sciencedirect.com/science/article/pii/S0921818106000142>. <https://doi.org/10.1016/j.gloplacha.2005.12.010>
- Banacos, P. C., & Schultz, D. M. (2005). The use of moisture flux convergence in forecasting convective initiation: Historical and operational perspectives. *Weather and Forecasting*, 20(3), 351–366. <https://doi.org/10.1175/WAF858.1>
- Biasutti, M., Voigt, A., Boos, W. R., Braconnot, P., Hargreaves, J. C., Harrison, S. P., et al. (2018). Global energetics and local physics as drivers of past, present and future monsoons. *Nature Geoscience*, 11(6), 392–400. <https://doi.org/10.1038/s41561-018-0137-1>
- Boisier, J. P., de Noblet-Ducoudré, N., Pitman, A. J., Cruz, F. T., Delire, C., van den Hurk, B. J. J. M., et al. (2012). Attributing the impacts of land-cover changes in temperate regions on surface temperature and heat fluxes to specific causes: Results from the first LUCID set of simulations. *Journal of Geophysical Research*, 117, D12116. <https://doi.org/10.1029/2011JD017106>
- Cleland, E. E., Cleland, E., Chuine, I., Menzel, A., Mooney, H., & Schwartz, M. (2007). Shifting plant phenology in response to global change. *Trends in Ecology & Evolution*, 22(7), 357–365. Available at: <http://www.sciencedirect.com/science/article/pii/S0169534707001309>. <https://doi.org/10.1016/j.tree.2007.04.003>
- Cook, B. I., Puma, M. J., & Krakauer, N. Y. (2011). Irrigation induced surface cooling in the context of modern and increased greenhouse gas forcing. *Climate Dynamics*, 37(7–8), 1587–1600. <https://doi.org/10.1007/s00382-010-0932-x>
- Cook, B. I., Shukla, S. P., Puma, M. J., & Nazarenko, L. S. (2015). Irrigation as an historical climate forcing. *Climate Dynamics*, 44(5–6), 1715–1730. <https://doi.org/10.1007/s00382-014-2204-7>
- de Noblet-Ducoudré, N., Boisier, J. P., Pitman, A., Bonan, G. B., Brovkin, V., Cruz, F., et al. (2012). Determining robust impacts of land-use-induced land cover changes on surface climate over North America and Eurasia: Results from the first set of LUCID experiments. *Journal of Climate*, 25(9), 3261–3281. <https://doi.org/10.1175/JCLI-D-11-00338.1>
- de Vrese, P., Hagemann, S., & Claussen, M. (2016). Asian irrigation, African rain: Remote impacts of irrigation. *Geophysical Research Letters*, 43, 3737–3745. <https://doi.org/10.1002/2016GL068146> [Accessed April 25, 2016]
- Defries, R. S., Bounoua, L., & Collatz, G. J. (2002). Human modification of the landscape and surface climate in the next fifty years. *Global Change Biology*, 8(5), 438–458. <https://doi.org/10.1046/j.1365-2486.2002.00483.x>
- Defries, R. S., Foley, J. A., & Asner, G. P. (2004). Land-use choice: Balancing human needs and ecosystem function. *Frontiers in Ecology and the Environment*, 2(5), 249–257. [https://doi.org/10.1890/1540-9295\(2004\)002\[0249:LCBNA\]2.0.CO;2](https://doi.org/10.1890/1540-9295(2004)002[0249:LCBNA]2.0.CO;2)
- Diffenbaugh, N. S. (2009). Influence of modern land cover on the climate of the United States. *Climate Dynamics*, 33(7), 945. <https://doi.org/10.1007/s00382-009-0566-z>
- Douglas, E. M., Beltrán-Przekurat, A., Niyogi, D., Pielke, R. A. Sr., & Vörösmarty, C. J. (2009). The impact of agricultural intensification and irrigation on land-Atmosphere interactions and Indian monsoon precipitation—A mesoscale modeling perspective. *Global and Planetary Change*, 67(1–2), 117–128. <https://doi.org/10.1016/j.gloplacha.2008.12.007>
- Douglas, E. M., Niyogi, D., Frrolking, S., Yeluripati, J. B., Pielke, R. A. Sr., Niyogi, N., et al. (2006). Changes in moisture and energy fluxes due to agricultural land use and irrigation in the Indian Monsoon Belt. *Geophysical Research Letters*, 33, L14403. <https://doi.org/10.1029/2006GL026550>
- Elliott, J., Deryng, D., Müller, C., Frieler, K., Konzmann, M., Gerten, D., et al. (2014). Constraints and potentials of future irrigation water availability on agricultural production under climate change. *Proceedings of the National Academy of Sciences*, 111(9), 3239–LP-3244. Available at: <http://www.pnas.org/content/111/9/3239.abstract>. <https://doi.org/10.1073/pnas.1222474110>
- Eyring, V., Bony, S., Meehl, G. A., Senior, C., Stevens, B., Stouffer, R. J., & Taylor, K. E. (2015). Overview of the Coupled Model Intercomparison Project Phase 6 (CMIP6) experimental design and organisation. *Geoscientific Model Development Discussion*, 8(12), 10,539–10,583. Available at: <http://www.geosci-model-dev-discuss.net/8/10539/2015/>. <https://doi.org/10.5194/gmdd-8-10539-2015>
- Eyring, V., Bony, S., Meehl, G. A., Senior, C. A., Stevens, B., Stouffer, R. J., & Taylor, K. E. (2016). Overview of the Coupled Model Intercomparison Project Phase 6 (CMIP6) experimental design and organization. *Geoscientific Model Development*, 9, 1937–1958.
- Feddema, J. J., Oleson, K. W., Bonan, G. B., Mearns, L. O., Buja, L. E., Meehl, G. A., & Washington, W. M. (2005). The importance of land-cover change in simulating future climates. *Science*, 310(5754), 1674–1678. <https://doi.org/10.1126/science.1118160>
- IPCC (2014). *Climate Change 2014: Impacts, Adaptation, and Vulnerability. Part A: Global and Sectoral Aspects. Contribution of Working Group II to the Fifth Assessment Report of the Intergovernmental Panel on Climate Change*. In C. B. Field et al. (Eds.). (1132 pp.). Cambridge, United Kingdom and New York, NY: Cambridge University Press.
- Findell, K. L., Berg, A., Gentile, P., Krasting, J. P., Lintner, B. R., Malyshev, S., et al. (2017). The impact of anthropogenic land use and land cover change on regional climate extremes. *Nature Communications*, 8(1), 989. <https://doi.org/10.1038/s41467-017-01038-w>
- Foley, J. A., Ramankutty, N., Brauman, K. A., Cassidy, E. S., Gerber, J. S., Johnston, M., et al. (2011). Solutions for a cultivated planet. *Nature*, 478(7369), 337. <https://doi.org/10.1038/nature10452-324>

- Freydank, K. & Siebert, S. (2008). Towards mapping the extent of irrigation in the last century: Time series of irrigated area per country.
- Friedl, M. A., Sulla-Menashe, D., Tan, B., Schneider, A., Ramankutty, N., Sibley, A., & Huang, X. (2010). MODIS collection 5 global land cover: Algorithm refinements and characterization of new datasets. *Remote Sensing of Environment*, 114(1), 168–182. <https://doi.org/10.1016/j.rse.2009.08.016>
- Friend, A. D., & Kiang, N. Y. (2005). Land surface model development for the GISS GCM: Effects of improved canopy physiology on simulated climate. *Journal of Climate*, 18(15), 2883–2902. <https://doi.org/10.1175/JCLI3425.1>
- Ge, J. (2010). MODIS observed impacts of intensive agriculture on surface temperature in the southern Great Plains. *International Journal of Climatology*, 30(13), 1994–2003. <https://doi.org/10.1002/joc.2093> [Accessed July 5, 2017]
- Gillett, N. P., Shiogama, H., Funke, B., Hegerl, G., Knutti, R., Matthes, K., et al. (2016). The Detection and Attribution Model Intercomparison Project (DAMIP v1.0) contribution to CMIP6. *Geoscientific Model Development*, 9(10), 3685–3697. <https://doi.org/10.5194/gmd-9-3685-2016>
- Giorgi, F., & Gutowski, W. J. (2015). Regional dynamical downscaling and the CORDEX initiative. *Annual Review of Environment and Resources*, 40(1), 467–490. <https://doi.org/10.1146/annurev-environ-102014-021217>
- Green, R. E., Cornell, S. J., Scharlemann, J. P., & Balmford, A. (2005). Farming and the fate of wild nature. *Science*, 307(5709), 550–LP-555. Available at: <http://science.sciencemag.org/content/307/5709/550.abstract>. <https://doi.org/10.1126/science.1106049>
- Greve, P., Gudmundsson, L., & Seneviratne, S. I. (2018). Regional scaling of annual mean precipitation and water availability with global temperature change. *Earth System Dynamics*, 9(1), 227–240. <https://doi.org/10.5194/esd-9-227-2018>
- Guimberteau, M., Laval, K., Perrier, A., & Polcher, J. (2012). Global effect of irrigation and its impact on the onset of the Indian summer monsoon. *Climate Dynamics*, 39(6), 1329–1348. <https://doi.org/10.1007/s00382-011-1252-5>
- Halder, S., Saha, S. K., Dirmeyer, P. A., Chase, T. N., & Goswami, B. N. (2016). Investigating the impact of land-use land-cover change on Indian summer monsoon daily rainfall and temperature during 1951–2005 using a regional climate model. *Hydrology and Earth System Sciences*, 20(5), 1765–1784. Available at: <http://www.hydrol-earth-syst-sci.net/20/1765/2016/> <https://doi.org/10.5194/hess-20-1765-2016> Accessed June 16, 2017
- Hirsch, A. L., Pitman, A. J., Kala, J., Lorenz, R., & Donat, M. G. (2015). Modulation of land-use change impacts on temperature extremes via land-atmosphere coupling over Australia. *Earth Interactions*, 19(12), 1–24. <https://doi.org/10.1175/EI-D-15-0011.1>
- Hirsch, A. L., Wilhelm, M., Davin, E. L., Thiery, W., & Seneviratne, S. I. (2017). Can climate-effective land management reduce regional warming? *Journal of Geophysical Research: Atmospheres*, 122, 2269–2288. <https://doi.org/10.1002/2016JD026125>
- Hirschi, M., Seneviratne, S. I., Alexandrov, V., Boberg, F., Boronean, C., Christensen, O. B., et al. (2011). Observational evidence for soil-moisture impact on hot extremes in southeastern Europe. *Nature Geoscience*, 4(1), 17–21. <https://doi.org/10.1038/ngeo1032>
- Hurt, G. C., Chini, L. P., Frolking, S., Betts, R. A., Feddema, J., Fischer, G., et al. (2011). Harmonization of land-use scenarios for the period 1500–2100: 600 years of global gridded annual land-use transitions, wood harvest, and resulting secondary lands. *Climatic Change*, 109(1–2), 117–161. <https://doi.org/10.1007/s10584-011-0153-2>
- Im, E.-S., Marcella, M. P., & Eltahir, E. A. B. (2013). Impact of potential large-scale irrigation on the West African monsoon and its dependence on location of irrigated area. *Journal of Climate*, 27(3), 994–1009. <https://doi.org/10.1175/JCLI-D-13-00290.1>
- Kharin, V. V., Flato, G. M., Zhang, X., Gillett, N. P., Zwiers, F., & Anderson, K. J. (2018). Risks from climate extremes change differently from 1.5°C to 2.0°C depending on rarity. *Earth's Future*, 6, 704–715. <https://doi.org/10.1002/2018EF000813>
- Kim, Y., Moorcroft, P. R., Aleinov, I., Puma, M. J., & Kiang, N. Y. (2015). Variability of phenology and fluxes of water and carbon with observed and simulated soil moisture in the Ent Terrestrial Biosphere Model (Ent TBM version 1.0.1.0.0). *Geoscientific Model Development*, 8(12), 3837–3865. <https://doi.org/10.5194/gmd-8-3837-2015>
- Koster, R. D. (2004). Regions of strong coupling between soil moisture and precipitation. *Science*, 305(5687), 1138–1140. Available at: <http://www.sciencemag.org/cgi/doi/10.1126/science.1100217>
- Kueppers, L. M., Snyder, M. A., & Sloan, L. C. (2007). Irrigation cooling effect: Regional climate forcing by land-use change. *Geophysical Research Letters*, 34, L03703. <https://doi.org/10.1029/2006GL028679>
- Lawrence, D. M., Hurtt, G. C., Arneth, A., Brovkin, V., Calvin, K. V., Jones, A. D., et al. (2016). The Land Use Model Intercomparison Project (LUMIP) contribution to CMIP6: Rationale and experimental design. *Geoscientific Model Development*, 9(9), 2973–2998. <https://doi.org/10.5194/gmd-9-2973-2016>
- Lee, E., Chase, T. N., Rajagopalan, B., Barry, R. G., Biggs, T. W., & Lawrence, P. J. (2009). Effects of irrigation and vegetation activity on early Indian summer monsoon variability. *International Journal of Climatology*, 29(4), 573–581. <https://doi.org/10.1002/joc.1721>
- Lee, E., et al. (2011). Simulated impacts of irrigation on the atmospheric circulation over Asia. *Journal of Geophysical Research*, 116, D08114. <https://doi.org/10.1029/2010JD014740>
- Lo, M. H., & Famiglietti, J. S. (2013). Irrigation in California's Central Valley strengthens the southwestern U.S. water cycle. *Geophysical Research Letters*, 40, 301–306. <https://doi.org/10.1002/rl.50108>
- Lobell, D. B., & Bonfils, C. (2008). The effect of irrigation on regional temperatures: A spatial and temporal analysis of trends in California, 1934–2002. *Journal of Climate*, 21(10), 2063–2071. <https://doi.org/10.1175/2007JCLI1755.1>
- Lobell, D. B., et al. (2008). Irrigation cooling effect on temperature and heat index extremes. *Geophysical Research Letters*, 35, L09705. <https://doi.org/10.1029/2008GL034145>
- Luyssaert, S., Jammet, M., Stoy, P. C., Estel, S., Pongratz, J., Ceschia, E., et al. (2014). Land management and land-cover change have impacts of similar magnitude on surface temperature. *Nature Climate Change*, 4(5), 389–393. <https://doi.org/10.1038/nclimate2196>
- Mahmood, R., Pielke, R. A. Sr., Hubbard, K. G., Niyogi, D., Dirmeyer, P. A., McAlpine, C., et al. (2014). Land cover changes and their biogeophysical effects on climate. *International Journal of Climatology*, 34(4), 929–953. <https://doi.org/10.1002/joc.3736>
- Matson, P. A., Parton, W. J., Power, A. G., & Swift, M. J. (1997). Agricultural intensification and ecosystem properties. *Science*, 277(5325), 504–LP-509. Available at: <http://science.sciencemag.org/content/277/5325/504.abstract>. <https://doi.org/10.1126/science.277.5325.504>
- Matthews, E. (1983). Global vegetation and land use: New high-resolution data bases for climate studies. *Journal of Climate and Applied Meteorology*, 22(3), 474–487. [https://doi.org/10.1175/1520-0450\(1983\)022<0474:GVALUN>2.0.CO;2](https://doi.org/10.1175/1520-0450(1983)022<0474:GVALUN>2.0.CO;2)
- McDermid, S. S., Mearns, L. O., & Ruane, A. C. (2017). Representing agriculture in Earth system models: Approaches and priorities for development. *Journal of Advances in Modeling Earth Systems*, 9, 2230–2265. <https://doi.org/10.1002/2016MS000749>
- Melillo, J. M., Terese, R., & Yohe, G. (Eds.) (2014). *Climate change impacts in the United States: The third national climate assessment*. U.S.: Global Change Research Program.
- Miller, R. L., Schmidt, G. A., Nazarenko, L. S., Tausnev, N., Bauer, S. E., DelGenio, A. D., et al. (2014). CMIP5 historical simulations (1850–2012) with GISS ModelE2. *Journal of Advances in Modeling Earth Systems*, 6, 441–478. <https://doi.org/10.1002/2013MS000266>
- Monfreda, C., Ramankutty, N., & Foley, J. A. (2008). Farming the planet: 2. Geographic distribution of crop areas, yields, physiological types, and net primary production in the year 2000. *Global Biogeochemical Cycles*, 22, GB1022. <https://doi.org/10.1029/2007GB002947>

- Mueller, N. D., Butler, E. E., McKinnon, K. A., Rhines, A., Tingley, M., Holbrook, N. M., & Huybers, P. (2015). Cooling of US Midwest summer temperature extremes from cropland intensification. *Nature Climate Change*, 6(3), 317–322. <https://doi.org/10.1038/nclimate2825>
- Mueller, N. D., Rhines, A., Butler, E. E., Ray, D. K., Siebert, S., Holbrook, N. M., & Huybers, P. (2017). Global relationships between cropland intensification and summer temperature extremes over the last 50 years. *Journal of Climate*, 30(18), 7505–7528. <https://doi.org/10.1175/JCLI-D-17-0096.1>
- Myhre, G., Shindell, D., Bréon, F.-M., Collins, W., Fuglestvedt, J., Huang, J., et al. (2013). Anthropogenic and natural radiative forcing (Chapter 8). In T. F. Stocker (Eds.), *Climate Change 2013: The Physical Science Basis. Contribution of Working Group I to the Fifth Assessment Report of the Intergovernmental Panel on Climate Change*. Cambridge, United Kingdom and New York, NY: Cambridge University Press.
- Nazarenko, L., Schmidt, G. A., Miller, R. L., Tausnev, N., Kelley, M., Ruedy, R., et al. (2015). Future climate change under RCP emission scenarios with GISS ModelE2. *Journal of Advances in Modeling Earth Systems*, 7, 244–267. <https://doi.org/10.1002/2014MS000403>
- Niyogi, D., Kishtawal, C., Tripathi, S., & Govindaraju, R. S. (2010). Observational evidence that agricultural intensification and land use change may be reducing the Indian summer monsoon rainfall. *Water Resources Research*, 46, W03533. <https://doi.org/10.1029/2008WR007082>
- Paul, S., Ghosh, S., Oglesby, R., Pathak, A., Chandrasekharan, A., & Ramsankaran, R. A. A. J. (2016). Weakening of Indian summer monsoon rainfall due to changes in land use/land cover. *Scientific Reports*, 6(1), 32177. <https://doi.org/10.1038/srep32177>
- Perugini, L., Caporaso, L., Marconi, S., Cescatti, A., Quesada, B., de Noblet-Ducoudré, N., et al. (2017). Biophysical effects on temperature and precipitation due to land cover change. *Environmental Research Letters*, 12(5), 053002. <http://stacks.iop.org/1748-9326/12/i=5/a=053002?key=crossref.c8fc6cd7f3570d3a8b7baf3fe79f149c>
- Pielke, R. A., Pitman, A., Niyogi, D., Mahmood, R., McAlpine, C., Hossain, F., et al. (2011). Land use/land cover changes and climate: Modeling analysis and observational evidence. *Wiley Interdisciplinary Reviews: Climate Change*, 2(6), 828–850.
- Pitman, A. J., de Noblet-Ducoudré, N., Cruz, F. T., Davin, E. L., Bonan, G. B., Brovkin, V., et al. (2009). Uncertainties in climate responses to past land cover change: First results from the LUCID intercomparison study. *Geophysical Research Letters*, 36, L14814. <https://doi.org/10.1029/2009GL039076>
- Pongratz, J., Reick, C., Raddatz, T., & Claussen, M. (2008). A reconstruction of global agricultural areas and land cover for the last millennium. *Global Biogeochemical Cycles*, 22, GB3018. <https://doi.org/10.1029/2007GB003153>
- Puma, M. J., & Cook, B. I. (2010). Effects of irrigation on global climate during the 20th century. *Journal of Geophysical Research*, 115, D16120. <https://doi.org/10.1029/2010JD014122>
- Puma, M. J., Koster, R. D., & Cook, B. I. (2013). Phenological versus meteorological controls on land-atmosphere water and carbon fluxes. *Journal of Geophysical Research: Biogeosciences*, 118, 14–29. <https://doi.org/10.1029/2012JG002088>
- Qian, Y., Huang, M., Yang, B., & Berg, L. K. (2013). A modeling study of irrigation effects on surface fluxes and land-air-cloud interactions in the southern Great Plains. *Journal of Hydrometeorology*, 14(3), 700–721. <https://doi.org/10.1175/JHM-D-12-0134.1>
- Quesada, B., Arneth, A., & de Noblet-Ducoudré, N. (2017). Atmospheric, radiative, and hydrologic effects of future land use and land cover changes: A global and multimodel climate picture. *Journal of Geophysical Research: Atmospheres*, 122, 5113–5131. <https://doi.org/10.1002/2016JD025448>
- Raddatz, R. L. (2007). Evidence for the influence of agriculture on weather and climate through the transformation and management of vegetation: Illustrated by examples from the Canadian prairies. *Agricultural and Forest Meteorology*, 142(2–4), 186–202. <https://doi.org/10.1016/j.agrformet.2006.08.022>
- Ramankutty, N., Evan, A. T., Monfreda, C., & Foley, J. A. (2008). Farming the planet: 1. Geographic distribution of global agricultural lands in the year 2000. *Global Biogeochemical Cycles*, 22, GB1003. <https://doi.org/10.1029/2007GB002952>
- Rayner, N. A., Parker, D. E., Horton, E. B., Folland, C. K., Alexander, L. V., Rowell, D. P., et al. (2003). Global analyses of sea surface temperature, sea ice, and night marine air temperature since the late nineteenth century. *Journal of Geophysical Research*, 108(D14), 4407. <https://doi.org/10.1029/2002JD002670>
- Rodell, M., Velicogna, I., & Famiglietti, J. S. (2009). Satellite-based estimates of groundwater depletion in India. *Nature*, 460(7258), 999–1002. <https://doi.org/10.1038/nature08238>
- Rosenzweig, C., & Abramopoulos, F. (1997). Land-surface model development for the GISS GCM. *Journal of Climate*, 10(8), 2040–2054. [https://doi.org/10.1175/1520-0442\(1997\)010%3C2040:LSMDFT%3E2.0.CO](https://doi.org/10.1175/1520-0442(1997)010%3C2040:LSMDFT%3E2.0.CO)
- Sacks, W. J., Cook, B. I., Buennning, N., Levis, S., & Helkowski, J. H. (2009). Effects of global irrigation on the near-surface climate. *Climate Dynamics*, 33(2–3), 159–175. <https://doi.org/10.1007/s00382-008-0445-z>
- Saeed, F., Hagemann, S., & Jacob, D. (2009). Impact of irrigation on the South Asian summer monsoon. *Geophysical Research Letters*, 36, L20711. <https://doi.org/10.1029/2009GL040625>
- Schmidt, G. A., Kelley, M., Nazarenko, L., Ruedy, R., Russell, G. L., Aleinov, I., et al. (2014). Configuration and assessment of the GISS ModelE2 contributions to the CMIP5 archive. *Journal of Advances in Modeling Earth Systems*, 6, 141–184. <https://doi.org/10.1002/2013MS000265>
- Seneviratne, S. I., Nicholls, N., Easterling, D., Goodess, C. M., Kanae, S., Kossin, J., et al. (2012). Changes in climate extremes and their impacts on the natural physical environment. In C. B. Field, et al. (Eds.), *Managing the risks of extreme events and disasters to advance climate change adaptation, a special report of Working Groups I and II of the Intergovernmental Panel on Climate Change (IPCC)* (pp. 109–230). Cambridge, United Kingdom and New York, NY, USA: Cambridge University Press.
- Seneviratne, S. I., Phipps, S. J., Pitman, A. J., Hirsch, A. L., Davin, E. L., Donat, M. G., et al. (2018). Land radiative management as contributor to regional-scale climate adaptation and mitigation. *Nature Geoscience*, 11(2), 88–96. <https://doi.org/10.1038/s41561-017-0057-5>
- Shukla, S. P., Puma, M. J., & Cook, B. I. (2014). The response of the South Asian summer monsoon circulation to intensified irrigation in global climate model simulations. *Climate Dynamics*, 42(1–2), 21–36. <https://doi.org/10.1007/s00382-013-1786-9>
- Taylor, K. E., Stouffer, R. J., & Meehl, G. A. (2011). An overview of CMIP5 and the experiment design. *Bulletin of the American Meteorological Society*, 93(4), 485–498. <https://doi.org/10.1175/BAMS-D-11-00094.1>
- Thiery, W., Davin, E. L., Lawrence, D. M., Hirsch, A. L., Hauser, M., & Seneviratne, S. I. (2017). Present-day irrigation mitigates heat extremes. *Journal of Geophysical Research: Atmospheres*, 122, 1403–1422. <https://doi.org/10.1002/2016JD025740>
- Tilman, D., Fargione, J., Wolff, B., D'Antonio, C., Dobson, A., Howarth, R., et al. (2001). Forecasting agriculturally driven global environmental change. *Science*, 292(5515), 281–LP-284. Available at: <http://science.scienmag.org/content/292/5515/281.abstract>. <https://doi.org/10.1126/science.1057544>
- Tuinenburg, O. A., Hutjes, R. W. A., Jacobs, C. M. J., & Kabat, P. (2011). Diagnosis of local land-atmosphere feedbacks in India. *Journal of Climate*, 24(1), 251–266. <https://doi.org/10.1175/2010JCLI379.1> [Accessed November 28, 2016]
- Tyagi, A., Sikka, D. R., Goyal, S., & Bhowmick, M. (2012). A satellite based study of pre-monsoon thunderstorms (Nor'westers) over eastern India and their organization into mesoscale convective complexes. *Mausam*, 63(1), 29–54.

- Wada, Y., van Beek, L. P. H., van Kempen, C. M., Reckman, J. W. T. M., Vasak, S., & Bierkens, M. F. P. (2010). Global depletion of groundwater resources. *Geophysical Research Letters*, 37, L20402. <https://doi.org/10.1029/2010GL044571>
- Wada, Y., Wisser, D., & Bierkens, M. F. P. (2014). Global modeling of withdrawal, allocation and consumptive use of surface water and groundwater resources. *Earth System Dynamics*, 5(1), 15–40. Available at: <http://www.earth-syst-dynam.net/5/15/2014/>. <https://doi.org/10.5194/esd-5-15-2014>
- Walther, G.-R., Post, E., Convey, P., Menzel, A., Parmesan, C., Beebee, T. J. C., et al. (2002). Ecological responses to recent climate change. *Nature*, 416(6879), 389–395. <https://doi.org/10.1038/416389a>
- Wey, H. W., Lo, M. H., Lee, S. Y., Yu, J. Y., & Hsu, H. H. (2015). Potential impacts of wintertime soil moisture anomalies from agricultural irrigation at low latitudes on regional and global climates. *Geophysical Research Letters*, 42, 8605–8614. <https://doi.org/10.1002/2015GL065883>
- Wilhelm, M., Davin, E. L., & Seneviratne, S. I. (2015). Climate engineering of vegetated land for hot extremes mitigation: An Earth system model sensitivity study. *Journal of Geophysical Research: Atmospheres*, 120, 2612–2623. <https://doi.org/10.1002/2014JD022293>
- Yamashima, R., Matsumoto, J., Takata, K., & Takahashi, H. G. (2015). Impact of historical land-use changes on the Indian summer monsoon onset. *International Journal of Climatology*, 35, 2419–2430.
- Yang, B., Zhang, Y., Qian, Y., Tang, J., & Liu, D. (2016). Climatic effects of irrigation over the Huang-Huai-Hai Plain in China simulated by the weather research and forecasting model. *Journal of Geophysical Research: Atmospheres*, 121, 2246–2264. <https://doi.org/10.1002/2015JD023736>
- Yang, Z., Dominguez, F., Zeng, X., Hu, H., Gupta, H., & Yang, B. (2017). Impact of irrigation over the California Central Valley on regional climate. *Journal of Hydrometeorology*, 18(5), 1341–1357. <https://doi.org/10.1175/JHM-D-16-0158.1>
- Zhang, W., Xu, Z., & Guo, W. (2016). The impacts of land-use and land-cover change on tropospheric temperatures at global and regional scales. *Earth Interactions*, 20(7), 1–23. <https://doi.org/10.1175/El-D-15-0029.1>
- Zhu, Z., Bi, J., Pan, Y., Ganguly, S., Anav, A., Xu, L., et al. (2013). Global data sets of vegetation leaf area index (LAI)3g and fraction of photosynthetically active radiation (FPAR)3g derived from global inventory modeling and mapping studies (GIMMS) normalized difference vegetation index (NDVI3G) for the period 1981 to 2. *Remote Sensing*, 5(2), 927–948. <https://doi.org/10.3390/rs5020927>